Inorg. Chem. **2007**, *46*, 10520–10533

Light-Induced Geometrical Changes in Acyclic Ruthenium(II) Complexes and Their Ruthena–Macrocyclic Analogues

Sylvestre Bonnet, Jean-Paul Collin,* and Jean-Pierre Sauvage

Laboratoire de Chimie Organo-Minérale, UMR 7177 du CNRS, Institut Le Bel, Université Louis Pasteur, 4 rue Blaise Pascal, 67000 Strasbourg Cedex, France

Received April 18, 2007

The two ligands **1** (4′-(3-anisylphenyl)-2,2′;6′,2″-terpyridine) and **2** (2-mesityl-8-anisyl-1,10-phenanthroline) (Scheme 2) were synthesized and coordinated to ruthenium. The corresponding complexes Ru(**1**)(**2**)(L)$^{n+}$, where L = Cl^-, CH_3CN, or C_5H_5N, have been fully characterized. Notably, the hindering mesityl group of the phenanthroline ligand was shown to lie opposite to the monodentate ligand L both in solution and in the solid state. Upon irradiation in acetonitrile or pyridine, quantitative isomerization of the complex occurred, which consisted of a 90° rotation of the bidentate chelate. In the new isomers the mesityl group was shown to π stack to the coordinated monodentate ligand with the anisyl group of the phen (1,10-phenanthroline) lying on the other side of the ruthenium atom. The back reaction was performed by heating the photochemical isomers of the complexes in DMSO and exchanging the DMSO with chloride anion, acetonitrile, or pyridine. The stability of the ruthenium(II)–pyridine bond was used in order to inscribe the Ru(terpy)(phen) motif in a molecular ring. Functionalization of the ligands and subsequent cyclization reaction on the complex were performed on the two isomers of Ru(**1**)(**2**)$(C_5H_5N)^{2+}$. Four macrocyclic complexes including the Ru(terpy)(phen)(py)$^{n+}$ moiety were obtained and characterized. A $(CH_2)_{18}$ alkane chain or polyethylene glycol chain formed the flexible part of the ruthena–macrocycles. Upon visible light irradiation a dramatic geometrical changeover of the cyclic complex took place, which could be reversed thermally.

Introduction

Control of discrete and large-amplitude motions via various types of signals is a key feature for the development of nanomechanical devices and information storage at the molecular level.[1−4] Photonic energy is particularly promising since this input signal can be switched on and off fast and readily on a very small place. Several molecular machines have recently been reported which are set in motion by light irradiation.[5−12] Among the light-driven molecular machine prototypes which have been described in the course of the past few years, a very distinct family of dynamic molecular systems takes advantage of the dissociative character of ligand-field states in Ru(diimine)$_3^{2+}$ complexes.[13−15] In these compounds, one part of the system is set in motion by photochemically expelling a given chelate, the reverse motion being performed simply by heating the product of the

(1) Balzani, V.; Venturi, M.; Credi, A. *Molecular Devices and Machines*; Wiley-VCH: Weinheim, 2003; p 494.
(2) Fabbrizzi, L.; Foti, F.; Patroni, S.; Pallavicini, P.; Taglietti, A. *Angew. Chem., Int. Ed.* **2004**, *43*, 5073.
(3) Balzani, V.; Credi, A.; Raymo, F. M.; Stoddart, F. J. A. *Angew. Chem., Int. Ed.* **2000**, *39*, 3348−3391.
(4) Sauvage, J.-P. *Molecular Machines and Motors*; Springer: Berlin, Heidelberg, 2001; Vol. 99.
(5) Ballardini, R.; Balzani, V.; Gandolfi, M.-T.; Prodi, L.; Venturi, M.; Philp, D.; Ricketts, H. G.; Stoddart, F. J. *Angew. Chem., Int. Ed.* **1993**, *32*, 1301−1303.
(6) Livoreil, A.; Sauvage, J.-P.; Armaroli, N.; Balzani, V.; Flamigni, L.; Ventura, B. *J. Am. Chem. Soc.* **1997**, *119*, 12114−12124.
(7) Armaroli, N.; Balzani, V.; Collin, J.-P.; Gavina, P.; Sauvage, J.-P.; Ventura, B. *J. Am. Chem. Soc.* **1999**, *121*, 4397−4408.
(8) Brouwer, A. M.; Frochot, C.; Gatti, F. G.; Leigh, D. A.; Mottier, L.; Paolucci, F.; Roffia, S.; Wurpel, G. W. H. *Science* **2001**, *291*, 2124−2128.
(9) Ashton, P. R.; Ballardini, R.; Balzani, V.; Credi, A.; Dress, K. R.; Ishow, E.; Kleverlaan, C. J.; Kocian, O.; Preece, J. A.; Spencer, N.; Stoddart, F. J.; Venturi, M.; Wenger, S. *Chem. Eur. J.* **2000**, *6*, 3558−3574.
(10) Murakami, H.; Kawabuchi, A.; Kotoo, K.; Kunitake, M.; Nakashima, N. *J. Am. Chem. Soc.* **1997**, *119*, 7605−7606.
(11) Eelkema, R.; Pollard, M. M.; Vicario, J.; Katsonis, N.; Serrano Ramon, B.; Bastiaansen, C. W. M.; Broer, D. J.; Feringa, B. L. *Nature* **2006**, *440*, 163.
(12) Balzani, V.; Clemente-Léon, M.; Credi, A.; Ferrer, B.; Venturi, M.; Flood, A. H.; Stoddart, J. F. *Proc. Natl. Acad. Sci. U.S.A.* **2006**, *103*, 1178−1183.
(13) Collin, J.-P.; Laemmel, A.-C.; Sauvage, J.-P. *New J. Chem.* **2001**, *25*, 22−24.
(14) Pomeranc, D.; Jouvenot, D.; Chambron, J.-C.; Collin, J.-P.; Sauvage, J.-P.; Heitz, V. *Chem. Eur. J.* **2003**, *9*, 4247−4254.
(15) Mobian, P.; Kern, J.-M.; Sauvage, J.-P. *Angew. Chem., Int. Ed.* **2004**, *43*, 2392−2395.

10.1021/ic700734q CCC: $37.00
Published on Web 11/15/2007

Scheme 1. Schematic View of the Two Ruthenium Isomer Complexes Displaying the Reorganization of the Flexible Chain Gathering the Ligands Terpyridine and Phenanthroline

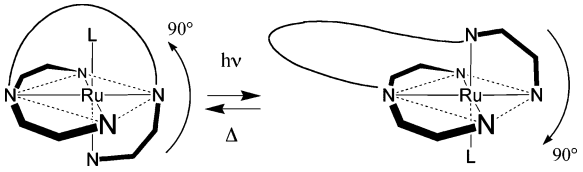

photochemical reaction so as to regenerate the original state. Complexes of the $[Ru(diimine)_3]^{2+}$ family are particularly well adapted to this approach. If distortion of the coordination octahedron is sufficient to significantly decrease the ligand field, which can be realized by using one or several sterically hindering ligands, the strongly dissociative ligand-field state (^{3}d−d state) can be efficiently populated from the metal-to-ligand charge-transfer (^{3}MLCT) state to result in expulsion of a given ligand. In a previously reported Ru(II) complex, a *p*-phenylene bridge linking two phen chelates blocked the coordination pattern of the complex during irradiations and enabled precise control of the geometry of the molecules.[16] In our quest to Ru(II)-containing macrocycles, we recently studied the $Ru(terpy)(phen)(L)^{2+}$ system, where L is a monodentate ligand (terpy = 2,2′;6′,2″-terpyridine and phen = 1,10-phenanthroline). This family of complexes allows the complexation of a wide variety of ligands L that can be photoexpelled upon light irradiation.[17−19] As rings are essential components of molecular machine prototypes and metal-templated catenanes and rotaxanes, we describe in the present report a new photoreactive system based on the $Ru(terpy)(phen)(L)^{n+}$ moiety embedded in a ring. This approach was not straightforward since the terpy fragment occupies three meridional sites of the octahedral coordination sphere and the phen chelate is orthogonal to the plane of the terpy. An alkyl or a polyethylene glycol chain as linker between a lateral position of the phen (3 position) and the para position (4′) of the central pyridine nucleus can gather these two fragments in a convenient way (Scheme 1).

Upon visible light irradiation, exchange of the monodentate ligand and isomerization take place in the ruthenium acyclic precursors, whereas additional dramatic contractions of the linkers were observed in the macrocyclic complexes. These photochemical reactions are generally thermally reversible with retention of the coordination geometry. A preliminary account of this work has been published recently.[20]

Results and Discussion

Since Ru(II) is kinetically inert, the so-called self-assembly approach could not be used to synthesize the targeted complexes and a strategy relying on organic chemistry

Scheme 2. Synthesis of Terpyridine **1** and Phenanthroline **2**

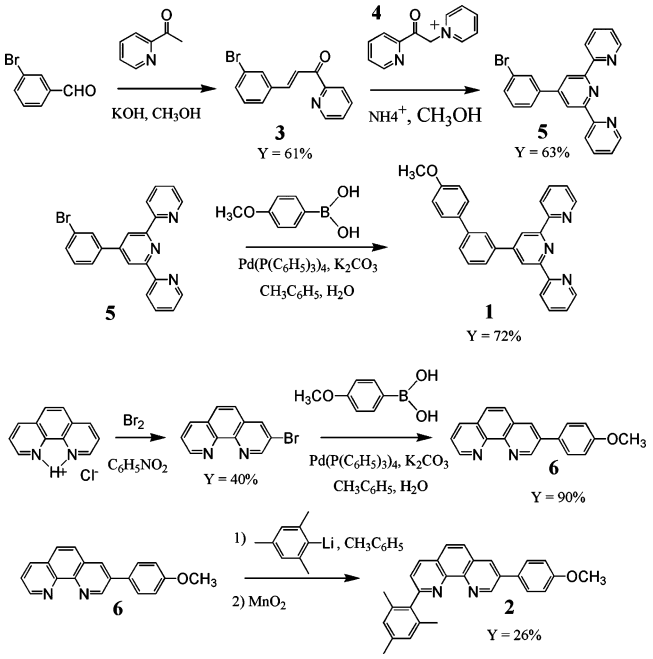

performed on the complex was adopted. The ruthenium precursor complexes should possess two chemically reactive functions favorably disposed in space. Two anisyl groups (as protected phenolic functions) have been introduced in appropriate positions of the terpyridine and phenanthroline. Use of a *m*-bromobenzaldehyde as precursor of the terpyridine leads, after a "Suzuki coupling" reaction, to a terpyridine displaying a first anchorage point for the linker. Another anisyl group introduced in the 8 position of the phenanthroline provides a second anchorage point without perturbing the ability of the coordination site of the ligand. Heteroleptic ruthenium complexes of the type $Ru(terpy)(phen)(L)^{n+}$ lead to two possible isomers if the bidentate ligand is unsymmetrical.[21] In an attempt to circumvent this difficulty a bulky mesityl group was introduced in the α position of one nitrogen atom of the phen. Synthesis of the ligands and the corresponding ruthenium complexes as well as their photochemical reactivity will be described in the first part of the article, while the second part will be devoted to the design, synthesis, and properties of the macrocyclic complexes incorporating the $Ru(terpy)(phen)(L)^{n+}$ moiety.

Synthesis of the Ligands and Their Corresponding Acyclic Complexes. The synthesis of the terpyridine **1** and phenanthroline **2** is shown in Scheme 2. Among the main synthetic methods toward terpyridines,[22,23] Kröhnke reaction was preferred for the synthesis of terpyridine **1** due to the mildness of the reaction conditions and simplicity of purification. Chalcone **3** and pyridinium iodide **4** were reacted in the presence of a nitrogen source (NH_4OCOCH_3) to generate, after air oxidation, the central pyridine ring of terpyridine **5**, which precipitated in the reaction mixture. A

(16) Mobian, P.; Kern, J.-M.; Sauvage, J.-P. *Helv. Chim. Acta* **2003**, *86*, 4195−4213.
(17) Bonnet, S.; Collin, J.-P.; Gruber, N.; Sauvage, J.-P. *J. Chem. Soc., Dalton Trans.* **2003**, 4654−4662.
(18) Bonnet, S.; Schofield, E. R.; Collin, J.-P.; Sauvage, J.-P. *Inorg. Chem.* **2004**, *43*, 8346−8354.
(19) Schofield, E. R.; Collin, J.-P.; Gruber, N.; Sauvage, J.-P. *Chem. Commun.* **2003**, 188−189.
(20) Bonnet, S.; Collin, J.-P.; Sauvage, J.-P. *Chem. Commun.* **2005**, 3195−3197.
(21) Laemmel, A.-C.; Collin, J.-P.; Sauvage, J.-P. *C. R. Acad. Sci. Paris* **2000**, *3*, 43−49.
(22) Heller, M.; Schubert, U. S. *Eur. J. Org. Chem.* **2003**, 947−961.
(23) Thompson, A. M. W. C. *Coord. Chem. Rev.* **1997**, *160*, 1−52.

Scheme 3. Synthesis of Ruthenium Complex $\mathbf{8_{th}}^{+}$

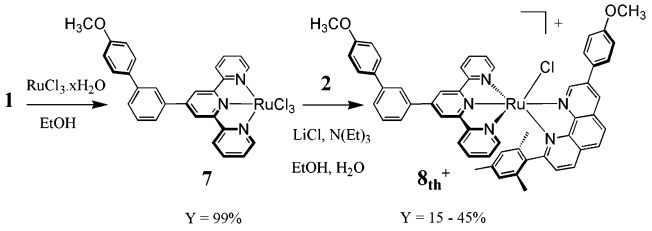

Suzuki cross-coupling reaction[24] between 4′-(3-bromophenyl)-2,2′;6′,2″-terpyridine (**5**) and commercially available anisylboronic acid resulted in terpyridine **1**.

Monobromination of 1,10-phenanthroline in the 3 position needs harsh conditions and was performed as the first step.[25] Although well described in the literature, this reaction was very sensitive to the reaction conditions and poorly reproducible. Notably, 3,5-dibromophenanthroline was often found as byproduct and difficult to remove by chromatography. A published recrystallization procedure was used in order to eliminate the dibrominated phenanthroline.[26] A Suzuki cross-coupling reaction between the monobrominated compound and anisylboronic acid leads to 3-anisyl-1,10-phenanthroline (**6**). Nucleophilic addition of lithiated derivatives, followed by rearomatization by manganese dioxide, is a very efficient method developed by Dietrich-Büchecker et al. for the introduction of aryl substituents in the α position to the nitrogen atom of polypyridine systems.[27] In the case of hindered derivatives like bromomesitylene, lithiation is performed at room temperature with *n*-BuLi.[28] Addition of the mesityllithium solution to the dissymmetric phenanthroline **6** in ether or toluene afforded, after rearomatization, a mixture of two regioisomers: 8-anisyl-2-mesityl-1,10-phenanthroline (**2**) and 3-anisyl-2-mesityl-1,10-phenanthroline. Separation on acidic alumina enabled isolation of both compounds in 26% and 19% yields, respectively.

The synthesis of the complex Ru(**1**)(**2**)(Cl)$^{+}$ ($\mathbf{8_{th}}^{+}$) is depicted in Scheme 3. As will be discussed later, two series of complexes have been obtained by either thermal or photochemical reactions. The origin of each complex will be mentioned by the abbreviations "th" and "photo", respectively, in lower index.

Coordination of terpyridine **1** on $RuCl_3 \cdot xH_2O$ was efficient and enabled gram-scale preparation of Ru(**1**)Cl_3 (**7**) as an insoluble brown material. Coordination of phenanthroline **2** to complex **7** was limiting in terms of reaction scale. With unhindered bidentate chelates like 2,2′-bipyridine or 1,10-phenanthroline, Calvert's conditions[29] gave the corresponding Ru(terpy)(N−N)(Cl)$^{+}$ complex in 60−70% yield.[17,18,30] In the case of phenanthroline **2**, metallic ruthenium and Ru(terpy)$_2^{2+}$ were also produced in relatively high yields, which limited the preparation of $\mathbf{8_{th}}^{+}$ in the 15−45% yield range. Separation of the two complexes $\mathbf{8_{th}}^{+}$ and Ru(terpy)$_2^{2+}$ was performed by chromatography on silica gel eluted with an acetone/water/aqueous saturated KNO_3 mixture (10:1:0.1). The electron-donating properties of the mesityl group in **2** as well as its hindering nature are suspected to be responsible for these limited yields. In addition, the selective obtention of the isomer $\mathbf{8_{th}}^{+}$ can be the consequence of the coordination, in a first process, of the nitrogen atom of the phenanthroline which is the less hindered. ROESY analysis on complex $\mathbf{8_{th}}^{+}$ showed that coordination of phenanthroline **2** to the ruthenium in complex Ru(**1**)Cl_3 was stereoselective. The only recovered complex was the isomer in which the monodentate chloride ligand is on the same side as the anisyl group of **2**.

Scheme 4. Thermal Ligand Substitution Reactions of $\mathbf{8_{th}}^{+}$

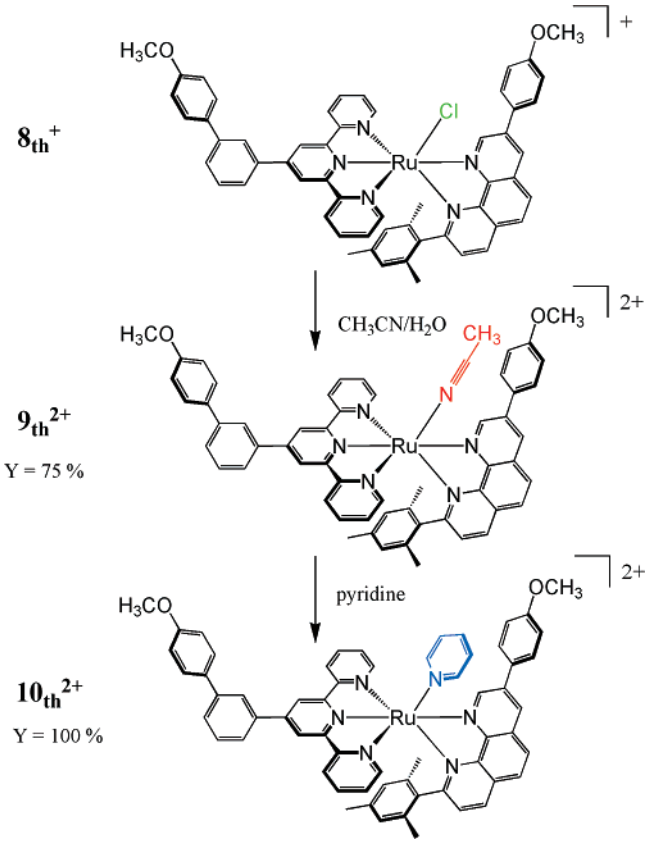

Chemical and Photochemical Reactivity of Complexes of the Type Ru(1)(2)(L)$^{n+}$. The chemical reactivity of Ru(**1**)(**2**)(L)$^{n+}$ complexes is in line with previously published work on related complexes (Scheme 4).[17,18,30]

Complex $\mathbf{8_{th}}^{+}$ reacted slowly in a refluxing acetonitrile−water mixture to afford complex $\mathbf{9_{th}}^{2+}$ in which the monodentate CH_3CN ligand was still on the side of the anisyl group. Heating of $\mathbf{9_{th}}^{2+}$ in pyridine at reflux leads quantitatively to complex $\mathbf{10_{th}}^{2+}$ in which pyridine is in the same position as acetonitrile in $\mathbf{9_{th}}^{2+}$. In both thermal reactions, the absence of light was critical to ensure retention of the geometrical coordination of the complexes. Suitable single crystals of $\mathbf{10_{th}}^{2+}$ were obtained by slow diffusion of an acetone solution of the complex into diisopropyl ether. The

(24) Miyaura, N.; Suzuki, A. *Chem. Rev.* **1995**, *95*, 2457−2483.
(25) Tzalis, D.; Tor, Y.; Failla, S.; Siegel, J. S. *Tetrahedron Lett.* **1995**, *36, (20)*, 3489−3490.
(26) Boldron, C.; Pitié, M.; Meunier, B. *Synlett* **2001**, *10*, 1629−1631.
(27) Dietrich-Buchecker, C.; Sauvage, J.-P. *Tetrahedron Lett.* **1982**, *23*, 5291−5294.
(28) Lüning, U.; Müller, M. *Chem. Ber.* **1990**, *123*, 643−645.
(29) Calvert, J. M.; Schmehl, R. H.; Sullivan, B. P.; Facci, J. S.; Meyer, T. J.; Murray, R. W. *Inorg. Chem.* **1983**, *22*, 2151−2162.
(30) Hecker, C. R.; Fanwick, P. E.; McMillin, D. R. *Inorg. Chem.* **1991**, *30*, 659−666.

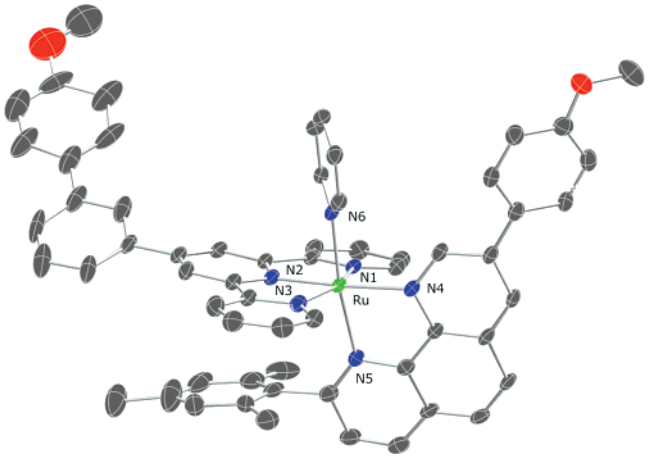

Figure 1. View of the crystal structure of the ruthenium complex $\mathbf{10}_{th}^{2+}$. Selected distances (Å) and angles (deg): Ru−N1 2.059(6), Ru−N2 1.965(6), Ru−N3 2.075(6), Ru−N4 2.076(6), Ru−N5 2.125(6), Ru−N6 2.097(6), N1−Ru−N2 79.9(2), N1−Ru−N3 158.9(2), N1−Ru−N4 95.2(2), N1−Ru−N5 86.3(2), N2−Ru−N3 79.1(2), N2−Ru−N4 174.5(2), N3−Ru−N4 105.8(2), N4−Ru−N6 92.5(2). H atoms and anions are omitted for clarity. Ellipsoids are scaled to enclose 50% of the electronic density.

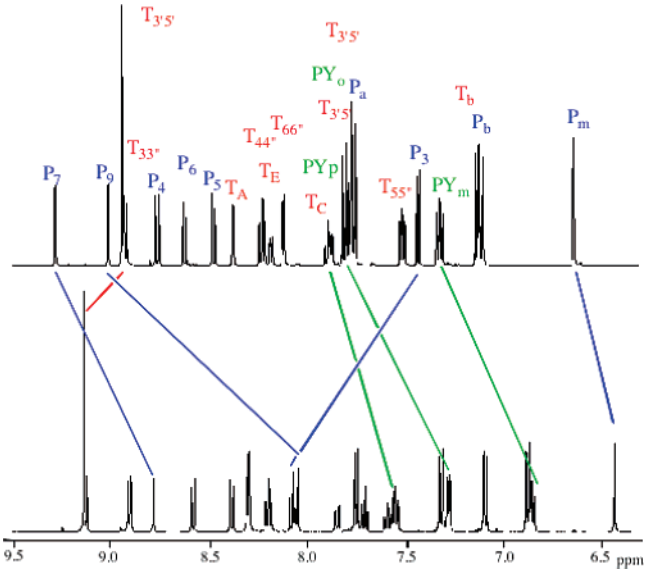

Figure 2. Proton NMR spectra of $\mathbf{10}_{th}^{2+}$ and $\mathbf{10}_{photo}^{2+}$ (aromatic region). (blue) Peaks of the phenanthroline. (red) Peaks of the terpyridine. (green) Peaks of the pyridine (noted PY). Scale is 9.5−6.3 ppm in acetone-d_6.

molecular crystallographic structure with partial numbering scheme is depicted Figure 1.

The bond lengths and N−Ru−N bond angles indicate that the geometry about the ruthenium atom is distorted from octahedral. In particular, a significant variation from the theoretical value is observed for the Ru−N5 bond length (2.12(6) Å) as a consequence of the steric constraint imposed by the mesityl substituent located in the α position of the nitrogen of the phenanthroline. The geometry in the solid state is also consistent with the ROESY interactions observed in solution. The mesityl group is located below the terpyridine moiety with π stacking between the central pyridine of the terpyridine and the mesityl aromatic cycle (average distance between the two cycles is 3.4 Å). On the other side of the ruthenium atom the pyridine ligand is close to the anisyl group belonging to the phenanthroline. The torsion angle O1−C20−C30−O2 is 45.71° and the two methoxy groups pointed toward the same side of the molecule, so that inclusion of this complex in a molecular ring could be envisaged (see below). The O1−O2 distance is 17.89 Å in this isomer.

Visible light irradiation of $\mathbf{10}_{th}^{2+}$ ($\lambda \geq 340$ nm) in neat pyridine leads to another species as demonstrated by UV−vis measurements (see Supporting Information) and ^{1}H NMR spectra (Figure 2) performed before and after irradiation.

As indicated by these spectra the photochemical reaction was selective and quantitative. The ES-MS spectrum also showed that the composition of the new complex is not changed. Complete assignment of the ^{1}H NMR spectrum by COSY and ROESY experiments clearly proves that $\mathbf{10}_{photo}^{2+}$ is an isomeric form of $\mathbf{10}_{th}^{2+}$ in which the mesityl group is close to the pyridine and far from the terpyridine (Scheme 5). A correlation peak was also detected in $\mathbf{10}_{th}^{2+}$ between the P_9 proton of the phenanthroline and the meta proton of the pyridine. Such a correlation peak is missing in $\mathbf{10}_{photo}^{2+}$, while two correlation peaks were observed between the

Scheme 5. Chemical Structures of Complexes $\mathbf{10}_{th}^{2+}$ and $\mathbf{10}_{photo}^{2+}$ [a]

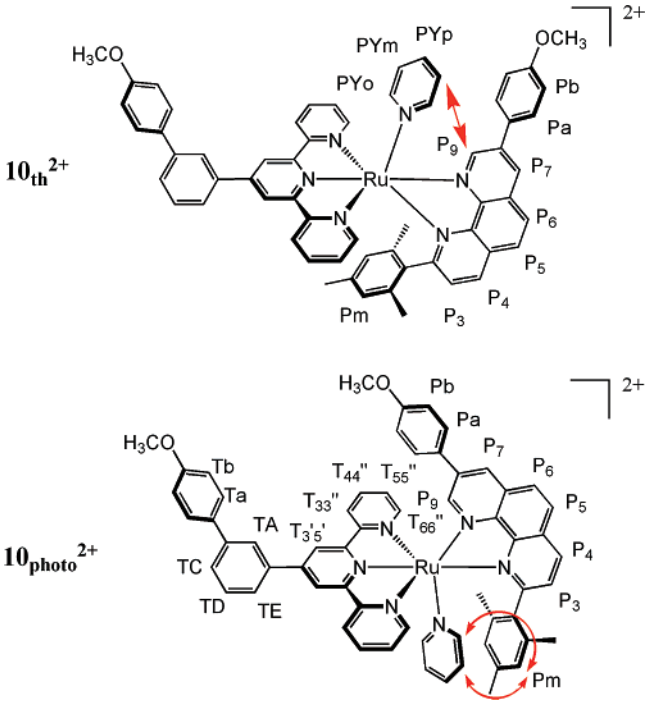

[a] Red arrows indicate selected ROESY interactions.

proton P_m of the mesityl group and the protons ortho and meta of the pyridine.

Irradiation of $\mathbf{9}_{th}^{2+}$ in acetonitrile leads to a similar photochemical isomerization since $\mathbf{9}_{th}^{2+}$ is quantitatively converted to isomer $\mathbf{9}_{photo}^{2+}$ in which the phenanthroline moiety rotated at a 90° angle and the acetonitrile ligand is on same the side as the mesityl group. This isomerization reaction was also directly carried out from complex $\mathbf{8}_{th}^{+}$ in acetonitrile/water and afforded in one quantitative step $\mathbf{9}_{photo}^{2+}$. In a similar manner, $\mathbf{9}_{th}^{2+}$ irradiated in pyridine directly afforded $\mathbf{10}_{photo}^{2+}$ with 100% yield. Scheme 6

Scheme 6. Photochemical Ligand Substitutions of Ru(**1**)(**2**)(L)$^{n+}$ Complexes

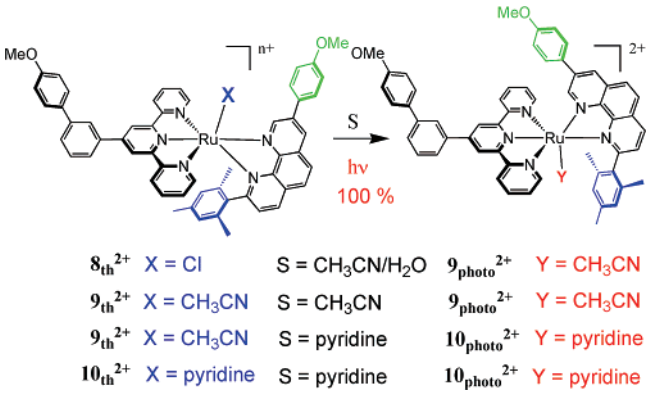

summarizes the photochemical ligand substitution pattern of Ru(**1**)(**2**)(L)$^{n+}$ complexes.

The two isomers (thermal and photochemical) of one particular complex have very similar UV−vis absorption spectra with a bathochromically shifted shoulder for the photochemical isomer that induced a slight color change after isomerization ($\mathbf{10_{th}}^{2+}$ was bright orange, whereas $\mathbf{10_{photo}}^{2+}$ was brownish). This shoulder was suspected to be caused by an intraligand $\pi-\pi^*$ charge-transfer transition from the donating mesityl group to the electron-deficient central ring of the terpyridine unit.

Chemical Reactivity of the Photochemically Produced Isomers. If the photochemical isomers of Ru(**1**)(**2**)(L)$^{n+}$ complex (L = CH_3CN or pyridine) are subjected to thermal ligand substitution reactions, ligand replacement of L generally leads to retention of the coordination geometry characteristic of the photochemical isomer. This was the case with pyridine, 3,5-dimethylpyridine, and benzonitrile, acting both as ligand and solvent. In the case of the chloride ion as entering ligand, in refluxing dichloroethane, a mixture of $\mathbf{8_{th}}^{+}$ and $\mathbf{8_{photo}}^{+}$ was obtained in a ratio of 13:87. In DMSO backisomerization to the thermal isomer was *quantitative*; in this process, pyridine was quantitatively removed, yielding the thermal S-bonded isomer Ru(**1**)(**2**)$(CH_3SOCH_3)^{2+}$ ($\mathbf{11_{th}}^{2+}$) and the thermal O-bonded isomer in a ratio of 90:10. These two products decompose on silica gel, but crude samples can be precipitated and isolated. Their study by ^{1}H NMR, electrospray mass spectrometry, and UV−vis absorption spectroscopy confirm the hypothesis of a mixture of S-bonded and O-bonded DMSO thermal isomers. The wavelength maxima at 437 and 490 nm are in agreement with the literature data,[31] and the peak in the mass spectrum at m/z = 499.642 (calcd 499.638) unambiguously proves the presence of a coordinated DMSO ligand.

Possible Mechanisms for the Thermal and Photochemical Reactions. From the experimental data two different mechanisms can be invoked independently in the thermal and photochemical reactions.

For the thermal reactions, at moderate temperature (<140 °C), an associative mechanism is in agreement with retention of the coordination geometry regardless of the structure of the starting isomer. For higher temperature, as in refluxing DMSO, it appears that the thermodynamic product can be obtained as the single product starting from the photochemical isomer.

For the photochemical reactions, a dissociative mechanism for this type of polypyridyl ruthenium(II) complexes has been well established in previous works.[30,32] Substitution of the monodentate ligand was supposed to be an elementary step occurring on the pentacoordinated species Ru(**1**)(**2**)$^{2+}$ generated by ligand L abstraction from the starting complex. Previous experimental data[19] and theoretical TD−DFT calculations[33] were consistent with such transient pentacoordinated species. Because of the dissymmetric substitution pattern of phenanthroline **2**, the two possible square-pyramidal five-coordinate intermediates do not have the same energy. As a consequence, steric hindrance due to the bulkiness of the mesityl group might be large enough to induce destabilization of a given five-coordinate intermediate as compared to the other. Considering that the bimolecular reaction between the pentacoordinated species and the entering ligand is a slow step at room temperature compared to the shift of the equilibrium between the five-coordinate transient species, the whole process would result in a 100% yield for the photochemical isomer at room temperature. The drastic effect of the mesityl group on the yield of the photochemical reaction is also in accordance with the results obtained with analogous ruthenium complexes in which the 3-anisyl-9-mesityl-1,10-phenanthroline has been replaced by the asymmetric 4-methyl-7-anisyl-1,10-phenanthroline. Visible light irradiation of any of the two possible thermal isomers leads to a statistical mixture (50:50) of two photochemical isomers. This photochemical behavior reflects the lack of a bulky group at the α position of a nitrogen atom of the phenanthroline. The details of these experiments are given in the Supporting Information.

Synthesis of Macrocycles Including the Ru(terpy)(phen)(py)$^{2+}$ Moiety. In the case of the Ru(phen)$_2$ core, Mobian et al. were able to synthesize a [2]-catenane by threading a 6,6′-dimethylbipyridine chelate bearing olefin-terminated chains inside a macrocycle containing a Ru(bisphen)Cl_2 unit followed by ring-closing metathesis.[16,34] Preliminary results showed that in the case of the Ru(terpy)(phen) core, coordination of terdentate, bidentate, or monodentate ligands bearing terminal olefins on a ruthenium center led to substantial polymerization and/or double-bond migration. Such processes prevented the isolation of any Ru(terpy)(phen)(L)$^{2+}$ complex surrounded by terminal olefins when starting from inorganic ruthenium salts and olefin-bearing free ligands. Another strategy toward macrocycles consisted of introducing the terminal olefins by performing organic chemistry on the periphery of ligands that were previously coordinated around ruthenium in a stable, saturated Ru(terpy)(phen)(py)$^{2+}$ complex. Reduction of all double bonds

(31) Rack, J. J.; Winkler, J. R.; Gray, H. B. *J. Am. Chem. Soc.* **2001**, *123*, 2432−2433.
(32) Suen, H.-F.; Wilson, S. W.; Pomerantz, M.; Walsh, J. L. *Inorg. Chem.* **1989**, *28*, 786−666791.
(33) Bossert, J. Ph.D. Thesis, Louis Pasteur University, Strasbourg, France, 2004.
(34) Arico, F.; Mobian, P.; Kern, J.-M.; Sauvage, J.-P. *Org. Lett.* **2003**, *5*, 1887−1890.

Scheme 7. Synthesis of the Precursor Complexes for the Grubbs Cyclization

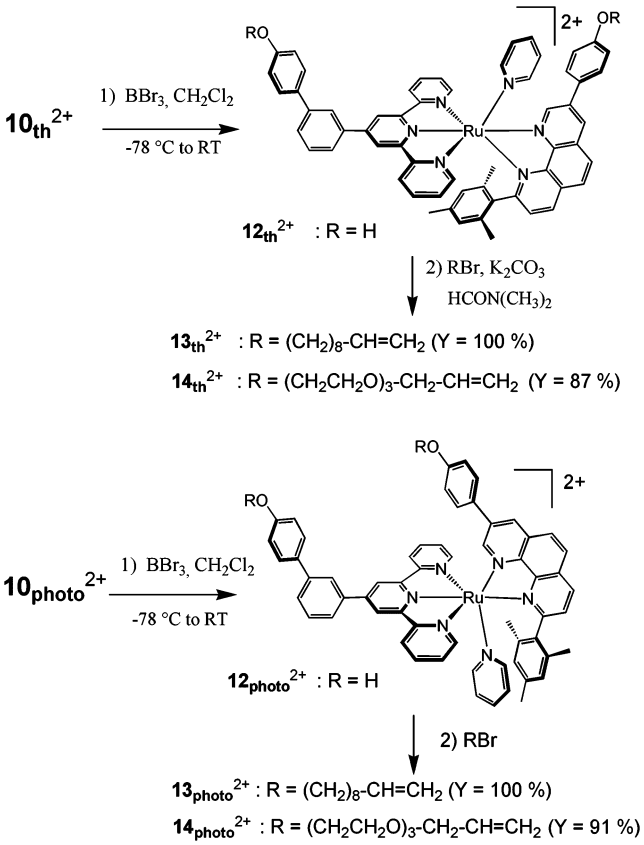

Scheme 8. Synthesis of the Thermally and Photochemically Reduced Ruthena−macrocycles

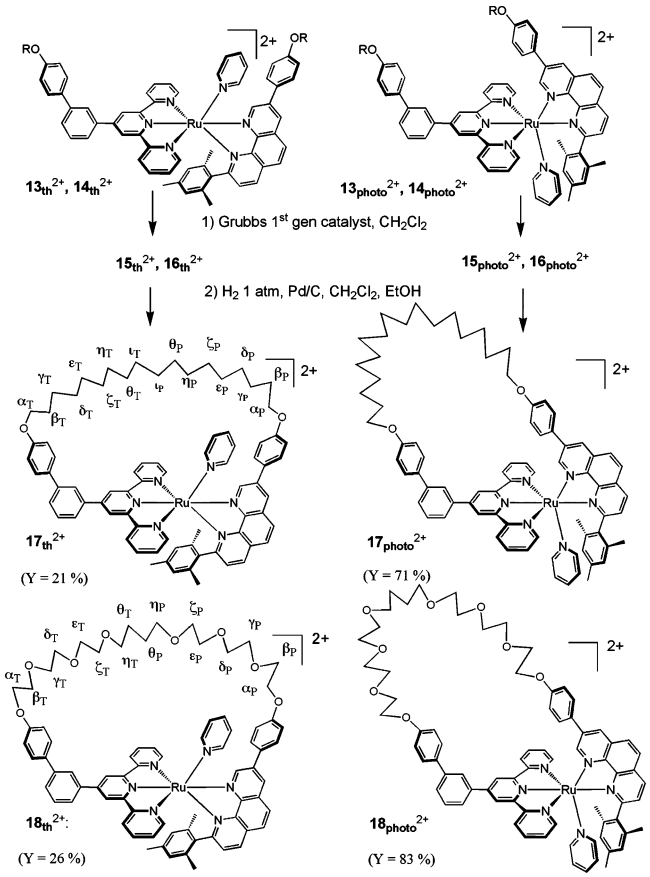

before any ligand-exchange experiments would be necessary. Complexes $\mathbf{10}_{\mathbf{th}}^{2+}$ and $\mathbf{10}_{\mathbf{photo}}^{2+}$ were used as starting material for inclusion of the Ru(terpy)(phen) core in macrocyclic species. Pyridine, being strongly coordinated to the Ru(terpy)(phen) core, acted as a protecting group for the monodentate coordination site. In these conditions, four organic reactions performed "on the complex" enabled the synthesis of macrocyclic species. (i) As a first step, boron tribromide deprotection of the methoxy groups in $\mathbf{10}_{\mathbf{th}}^{2+}$ and $\mathbf{10}_{\mathbf{photo}}^{2+}$ quantitatively afforded the phenol complexes $\mathbf{12}_{\mathbf{th}}^{2+}$ and $\mathbf{12}_{\mathbf{photo}}^{2+}$, respectively. (ii) Subsequent alkylation using alkane or poly(ethylene glycol) chains in Williamson conditions afforded the four precursor complexes $\mathbf{13}_{\mathbf{th}}^{2+}$, $\mathbf{14}_{\mathbf{th}}^{2+}$, $\mathbf{13}_{\mathbf{photo}}^{2+}$, and $\mathbf{14}_{\mathbf{photo}}^{2+}$ bearing terminal olefins (Scheme 7). (iii) Grubbs' first-generation olefin metathesis reactions were used as the cyclization step. As is generally the case for this reaction,[35] the geometry of the precursor was a critical parameter for preparation of monomeric macrocycles. A priori, the geometry of the photoisomers ($\mathbf{13}_{\mathbf{photo}}^{2+}$ or $\mathbf{14}_{\mathbf{photo}}^{2+}$) is much more favorable to formation of a ring than that of its thermal analogue. As expected, the thermal and photochemical isomers reacted very differently: in the case of the thermal isomers, 5−7 days were needed to complete the reaction. The monomer yields were low, typically around 25%, and an appreciable amount of the dimer was isolated and clearly identified by electrospray mass spectrometry. In the case of the photochemical isomers, the reaction was finished within 2 days and led to a single major product analyzed by ES-MS as the monomeric macrocycle in 70−80% yield. (iv) In order to avoid unexpected side reactions on the olefin function during photoinduced or thermal ligand substitution reactions on the Ru(terpy)(phen)(L)$^{n+}$ macrocyclic complexes, $\mathbf{15}^{2+}$ and $\mathbf{16}^{2+}$ were reduced by hydrogenation over Pd/C. This last catalytic step quantitatively afforded the four corresponding macrocycles with a $(CH_2)_{18}$ alkane chain ($\mathbf{17}_{\mathbf{th}}^{2+}$ and $\mathbf{17}_{\mathbf{photo}}^{2+}$) or a $(CH_2CH_2O)_3-(CH_2)_4-(CH_2CH_2O)_3$ polyethylene glycol chain ($\mathbf{18}_{\mathbf{th}}^{2+}$ and $\mathbf{18}_{\mathbf{photo}}^{2+}$). The last two steps are described in Scheme 8. ROESY studies clearly showed that in $\mathbf{17}_{\mathbf{th}}^{2+}$ and $\mathbf{18}_{\mathbf{th}}^{2+}$ the pyridine monodentate ligand was located inside the macrocyclic cavity, whereas in $\mathbf{17}_{\mathbf{photo}}^{2+}$ and $\mathbf{18}_{\mathbf{photo}}^{2+}$ it was outside the macrocycle.

Interconversion between Thermal and Photochemical Macrocycles. The macrocyclic ruthenium complexes $\mathbf{17}_{\mathbf{th}}^{2+}$, $\mathbf{18}_{\mathbf{th}}^{2+}$, $\mathbf{17}_{\mathbf{photo}}^{2+}$, and $\mathbf{18}_{\mathbf{photo}}^{2+}$ have been submitted to the same reaction conditions as their acyclic counterparts $\mathbf{10}_{\mathbf{th}}^{2+}$ and $\mathbf{10}_{\mathbf{photo}}^{2+}$. These experiments unambiguously led to the same results as in the case of the acyclic complexes and without noticeable difference between the alkane or poly(ethylene glycol) (PEG) chains. Irradiation of the thermal isomers in pyridine led quantitatively to ligand exchange *and* isomerization. Thermal back-isomerization only took place in dimethyl sulfoxide at 140 °C for 2 h, all other solvents (acetonitrile, pyridine, 3,5-lutidine, or benzonitrile) leading to ligand substitution *without* back-isomerization. DMSO,

(35) Belfrekh, N.; Dietrich-Buchecker, C.; Sauvage, J.-P. *Inorg. Chem.* **2000**, *39*, 5169−5172.

Scheme 9. Square Reaction Scheme Leading To Interconversion between the Photochemical and Thermal Isomers

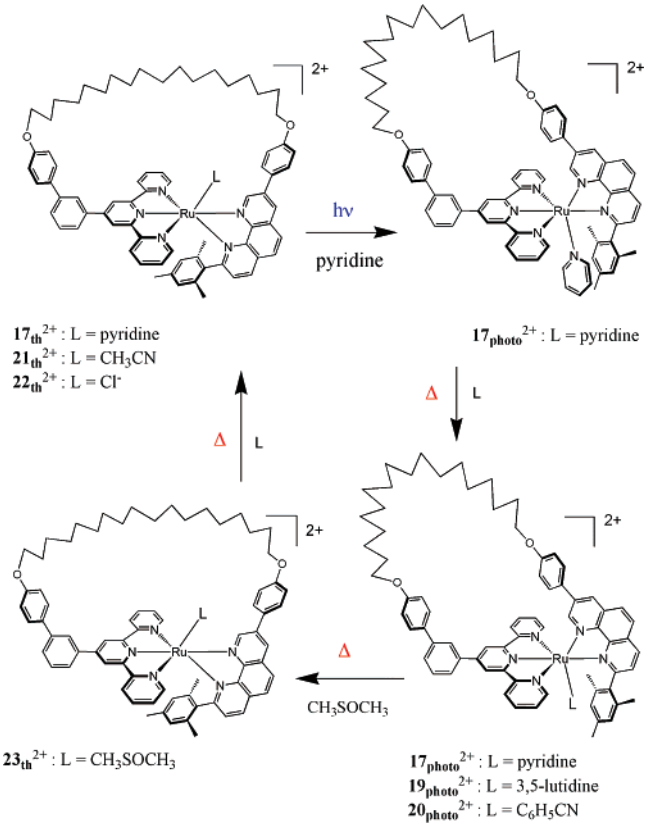

being only weakly coordinated to the ruthenium center in the thermal isomers of the macrocyclic complexes, thermal ligand exchange in refluxing pyridine, acetonitrile, or dichloromethane solution of tetraethylammonium chloride, afforded the corresponding thermal macrocycle with a pyridine, acetonitrile, or chloride ligand inside the macrocyclic cavity. The interconversion scheme in the case of the $(CH_2)_{18}$ alkane chain is depicted in Scheme 9 (photochemical macrocycles with L = 3,5-dimethylpyridine and benzonitrile are denoted $\mathbf{19}_{\mathbf{photo}}^{2+}$ and $\mathbf{20}_{\mathbf{photo}}^{2+}$, respectively; thermal macrocycles with L = acetonitrile, chloride, and DMSO are denoted $\mathbf{21}_{\mathbf{th}}^{2+}$, $\mathbf{22}_{\mathbf{th}}^{2+}$, and $\mathbf{23}_{\mathbf{th}}^{2+}$, respectively).

Analysis of the Conformations of the Flexible Chains. In the crystal structure of $\mathbf{10}_{\mathbf{th}}^{2+}$ the O1−O2 distance was 17.89 Å. Chem3D molecular modeling calculations predicted that this distance could be shortened by rotation of the C8−C16 single bond. The minimum value of 15.9 Å was obtained in the conformer where the directions of the two anisyl groups were included in the plane of the phenanthroline. Unfortunately $\mathbf{10}_{\mathbf{photo}}^{2+}$ could not be crystallized, but the same molecular modeling analysis performed on this isomer gave as the shortest value 6.3 Å. Keeping in mind that molecular modeling gives only an evaluation of the distances, this analysis would imply that the O1−O2 distance in the thermal isomer was two to three times longer than that in the photochemical isomer.

In complexes $\mathbf{17}^{2+}$ and $\mathbf{18}^{2+}$ where a flexible chain has been attached to these oxygen atoms, the huge variation of the O1−O2 distance induced by the 90° rotation of the phenanthroline moiety may lead to a dramatic change in the

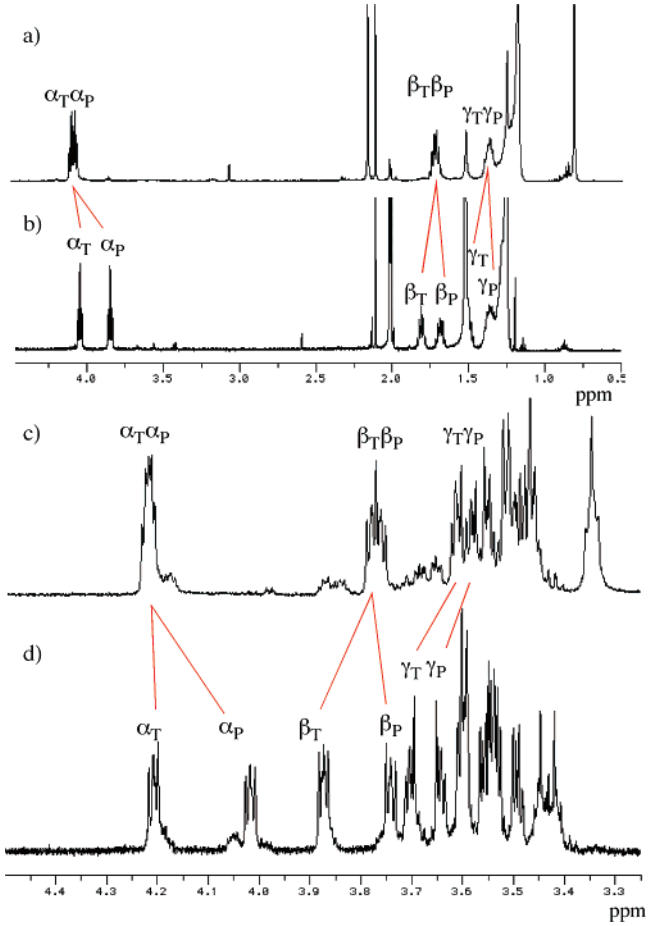

Figure 3. ^{1}H 500 MHz NMR spectra of the alkane chains in $\mathbf{17}_{\mathbf{th}}^{2+}$ and $\mathbf{17}_{\mathbf{photo}}^{2+}$ (a and b, respectively) and the polyethylene glycol chains in $\mathbf{18}_{\mathbf{th}}^{2+}$ and $\mathbf{18}_{\mathbf{photo}}^{2+}$ (c and d, respectively).

conformation of the chain. NMR spectroscopy could, in principle, measure the difference in chain mobility between thermal and photochemical macrocyclic complexes. Figure 3a and b depicts the change of the alkane region (4.5−0.5 ppm in CD_2Cl_2) of the NMR spectrum of $\mathbf{17}_{\mathbf{th}}^{2+}$ and $\mathbf{17}_{\mathbf{photo}}^{2+}$, and Figure 3c and d gives the corresponding analysis in the ether region for $\mathbf{18}_{\mathbf{th}}^{2+}$ and $\mathbf{18}_{\mathbf{photo}}^{2+}$ (4.5−3.25 ppm in CD_2Cl_2, see Scheme 8 for proton assignments). Obvious broadening of the peaks was observed in $\mathbf{17}_{\mathbf{th}}^{2+}$ and $\mathbf{17}_{\mathbf{photo}}^{2+}$ going from α_T,α_P to γ_T,γ_P, which demonstrated that the conformations close to the aromatic anchors were well fixed, whereas in the middle of the chain the number of available conformations was very high. As can be seen in Figure 3, the dissymmetry of the ring in the thermal isomers $\mathbf{17}_{\mathbf{th}}^{2+}$ and $\mathbf{18}_{\mathbf{th}}^{2+}$ was weakly pronounced, and most of the CH_2 signals of the side of the phen and of the side of the terpy had similar chemical shifts. This resulted in a lack of resolution that prevented any quantitative conformational analysis based on coupling constants. By contrast, in the photochemical isomers $\mathbf{17}_{\mathbf{photo}}^{2+}$ and $\mathbf{18}_{\mathbf{photo}}^{2+}$, both sides (phen and terpy) were clearly distinguished, except in the 1.0−1.5 ppm region for $\mathbf{17}_{\mathbf{photo}}^{2+}$ where the resolution was still too low. In these isomers the dissymmetric nature of the macrocycles obviously appeared. However, the ^3J coupling constants for the α_T,α_P, β_T,β_P, and γ_T,γ_P peaks in $\mathbf{17}_{\mathbf{th}}^{2+}$ and $\mathbf{17}_{\mathbf{photo}}^{2+}$ were not conclusive, and the inherent complexity of the signals

in $\mathbf{18}_{\mathbf{photo}}^{2+}$ prevented us from running quantitative conformational analysis. Despite this lack of quantitative data, the spectra in Figure 3 qualitatively demonstrate the dramatic geometrical changeover of the macrocycles when changing from the thermal isomers to the photochemical ones.

Conclusion

The two chelates **1** and **2** in which **1** is a terpyridine derivative and **2** is a 2,8 dissymmetrically substituted 1,10-phenanthroline were synthesized and coordinated to ruthenium(II). The corresponding series of complexes with the formula Ru(**1**)(**2**)(L)$^{n+}$ displayed a classical reactivity under thermal ligand-exchange conditions with L = Cl^-, CH_3CN, or C_5H_5N. However, a novel isomerization phenomenon consisting of a quantitative 90° rotation of the phenanthroline moiety took place at room temperature under visible light irradiation. The reverse motion was shown to take place only by heating the complex in dimethyl sulfoxide at 140 °C for 2 h. Although photoisomerization of double bonds is a classic in photochemistry, photoinduced isomerization inside the coordination sphere of a ruthenium atom has not been reported much.[36] In $Ru(bpy)_2(OH_2)_2^{2+}$ indeed, trans−cis and cis−trans isomerization occur via the pentacoordinated species derived from the starting complex by photoexpulsion of H_2O. This system was characterized by a trans/cis ratio of 3:2 at the photostationary state. In the system described in the present paper, photoinduced conversion to the photochemical isomer was quantitative. Although quantitative calculation would be needed for a more complete understanding of this system, an analysis based on the interactions between the mesityl group of phenanthroline **2** and (i) terpyridine **1** bearing a phenyl substituent in 4′ position or (ii) the monodentate ligand L′ entering into the coordination sphere of the ruthenium during the substitution reaction is proposed.

Unlike flexible nitrogen-, sulfur-, or phosphorus-bearing ligands,[37,38] alkane chains cannot be preorganized by metal−heteroatoms interactions, and oxygen-bearing polyethylene glycol chains (PEG) coordinate to metals only in the presence of cooperative effects like in crown ether or cavitands.[39] As a result, controlling the conformations of long alkanes or acyclic PEG chains is difficult and can be only realized by using stiff elements that force the chain to adopt a given set of conformations. Some interesting experimental results have been obtained by enclosure of alkanes or PEG chains inside self-assembled molecular cages,[40−43] by packing them on metal surfaces like corn ears in a corn field,[44] or by wrapping the chains in a helical fashion around polyalkyne wires through metal-templated synthesis.[45] However, to our knowledge, switching processes controlled by an external signal and inducing a major conformational change of a flexible chain has not been achieved yet.

In this work, a stiff Ru(terpy)(phen) subunit was inscribed in a molecular ring by organic chemistry performed on the two isomers of complex Ru(**1**)(**2**)(py)$^{2+}$. In order to connect the terpy unit and the phen motif, an alkane and a poly(ethylene glycol) chain have been used. In both cases, the photochemically induced isomerization of the ruthenium complex and the reverse thermal reaction in DMSO were observed with no change compared to the acyclic species. This controlled rotation motion of the phenanthroline moiety around ruthenium induced a major change in the conformations of the flexible chains. Such high-yield conformational reorganization was performed due to the 2- to 3-fold variation of the distance between the two oxygen atoms hooking the extremities of the molecular string to the complex. In parallel, the monodentate pyridine ligand located outside the ring in the photochemical isomer moved to an intracavity position in the thermal isomer. The thermal macrocycles including the Ru(terpy)(phen)(CH_3CN)$^{2+}$ moiety with the monodentate coordination site *inside* the ring will be used in future metal-templated synthesis of interlocking molecules like [2]-catenanes and rotaxanes.

Experimental Section

Single-crystal X-ray diffraction experiments were carried out using Kappa CCD and graphite-monochromated Mo Kα radiation (λ = 0.71073 Å). For all computations the MolEN package was used,[46] and structures were drawn using CRYSTALMAKER. ^{1}H NMR spectra were acquired on either a Bruker AVANCE 300 (300 MHz), Bruker AVANCE 400 (400 MHz), or Bruker AVANCE 500 (500 MHz) spectrometer using the deuterated solvent as the lock and residual solvent as the internal reference. Mass spectra were obtained using a VG ZAB-HF(FAB) spectrometer, a VG-BIOQ triple quadrupole, positive mode, or a Bruker MicrOTOF spectrometer (ES-MS). UV−vis spectra were recorded with a Kontron Instruments UVIKON 860 spectrometer at room temperature.

(2(2-Bromoethoxy)ethoxy)ethyl allyl ether was prepared according to the literature procedure[34] using lithium bromide instead of sodium iodide. Pyridine was distilled and kept over KOH under argon. Dimethyl sulfoxide was distilled and kept under argon. Ammonium acetate and tetraethylammonium chloride were commercial product dried overnight under vacuum. 1,10-Phenanthroline hydrochloride, paramethoxyphenyl boronic acid, palladium tetrakis(triphenylphosphine), 3,5-lutidine, benzonitrile, acetonitrile, 3-bromobenzaldehyde, 2-acetylpyridine, 10-bromo-dec-1-ene, 2-bromomesitylene, and Grubbs' first-generation catalyst were commercial products. $RuCl_3 \cdot xH_2O$ was kindly provided by Johnson Matthey Inc. Dichloromethane was distilled under CaH_2. Tetrahydrofuran,

(36) Durham, B.; Wilson, S. W.; Hodgson, D. J.; Meyer, T. J. *J. Am. Chem. Soc.* **1980**, *102*, 600−607.
(37) Piguet, C.; Borkovec, M.; Hamacek, J.; Zeckert, K. *Coord. Chem. Rev.* **2005**, *249*, 705−726.
(38) Swiegers, G. F.; Malefetse, T. J. *Chem. Rev.* **2000**, *100*, 3483−3537.
(39) Lehn, J.-M. *La Chimie Supramoléculaire-concepts et perspectives*; De Boeck Université: Brussels, Belgium, 1997; p 273.
(40) Trembleau, L.; Rebek, J., Jr. *Science* **2003**, *301*, 1219−1220.
(41) Scarso, A.; Trembleau, L.; Rebek, J., Jr. *J. Am. Chem. Soc.* **2004**, *126*, 13512−13518.
(42) Scarso, A.; Trembleau, L.; Rebek, J., Jr. *Angew. Chem., Int. Ed.* **2003**, *42*, 5499−5502.
(43) Love, J. C.; Wolfe, D. B.; Haasch, R.; Chabinyc, M. L.; Paul, K. E.; Whitesides, G. M.; Nuzzo, R. G. *J. Am. Chem. Soc.* **2003**, *125*, 2597−2609.
(44) Love, J. C.; Estroff, L. A.; Kriebel, J. K.; Nuzzo, R. G.; Whitesides, G. M. *Chem. Rev.* **2005**, *105*, 1103−1169.
(45) Stahl, J.; Bohling, J. C.; Bauer, E. B.; Peters, T. B.; Mohr, W.; Martin-Alvarez, J. M.; Hampel, F.; Gladysz, J. A. *Angew. Chem., Int. Ed.* **2002**, *41*, 1871−1876.
(46) Fair, C. K. *MolEN, An interactive intelligent system for crystal structure analysis*; Nonius: Delft, The Netherlands, 1990.

diethyl ether, and toluene were distilled and dried over sodium. Acetone was distilled and dried over sodium sulfate. KPF_6 was used as a 40 g/L aqueous solution. KNO_3 was used as a saturated aqueous solution. In every synthesis of ruthenium complexes chromatography fractions were worked up as follows: addition of an excess amount of KPF_6, evaporation of the organic solvent (acetone or acetonitrile) until precipitation, filtration, washing with water, recovery from the frit with acetone, and drying under vacuum.

1. A 1.16 g (3.0 mmol) amount of 4′-(3-bromophenyl)terpyridine was dissolved in 100 mL of toluene in a three-necked 250 mL round-bottom flask. The flask was put under argon; 173 mg (150 μmol, 5 mol %) of palladium tetrakis(triphenylphosphine) was added under argon. A 20 mL amount of 2 M degassed sodium carbonate aqueous solution was cannulated, followed by 502 mg (3.30 mmol) of *p*-anisylphenyl boronic acid dissolved in 50 mL of toluene and 8 mL of ethanol. The reaction mixture was degassed and refluxed under argon overnight. The solvents were evaporated, and water was added and extracted with dichloromethane. The organic phase was washed once with water and evaporated. The product was purified on neutral alumina (200 mL) using a 3:7 to 35:15 diethyl ether/pentane mixture as the eluent. Yield: 879 mg of terpyridine **1** (71%). ^{1}H 500 MHz NMR (δ in ppm in $CDCl_3$): 8.79 (s, 2H, T3′5′); 8.73 (m, 2H, T66″); 8.68 (dt, 2H, T33″, J = 7.9,1.1 Hz); 8.05 (t, 1H, TA, J = 1.8 Hz); 7.88 (td, 2H, T44″, J = 7.7, 1.8 Hz); 7.82 (m, 1H, TE); 7.64−7.61 (m, 3H, TC + Ta); 7.56 (t, 1H, TD, J = 7.7 Hz); 7.35 (m, 2H, T55″); 7.02 (d, 2H, Tb, J = 8.8 Hz); 3.87 (s, 3H, OMe). HR FAB MS *m*/*z* (calcd): 416.1769 (416.1762, $[M + H]^+$). Anal. Calcd for $C_{28}H_{21}N_3O$: C, 80.94; H, 5.09; N, 10.11. Found: C, 80.69; H, 5.17; N, 10.03.

2. A 434 mg (2.18 mmol) amount of mesityl bromide was put under argon in a 100 mL round-bottom flask. A 50 mL amount of dry diethyl ether was cannulated, 1.57 mL of *n*-butyllithium (1.37 M, 2.15 mmol) was added, and the mixture was stirred under argon for 5 h. In a three-necked 250 mL round-bottom flask, 513 mg of 3-anisylphenanthroline was weighed and dissolved in 150 mL of dry diethyl ether or toluene under argon. The ether solution of aryllithium was dropwise cannulated at room temperature into the reaction flask, leading to a fast color change from colorless to deep violet. The solution was stirred under argon at room temperature for 20 h and quenched with 25 mL of water. The solvents were evaporated, and water was added and extracted with dichloromethane. To the combined yellow dichloromethane extracts was added 10 equiv (1.6 g) of manganese dioxide. The solution was stirred at room temperature for 5 min, and this procedure was repeated twice again. The manganese oxide was filtered on celite, and the clear solution was evaporated to dryness, yielding 728 mg of re-aromatized crude product. The two phenanthroline regioisomers were separated on acidic alumina (200 mL) using a 20:2:2 pentane/dichloromethane/ethylacetate mixture as the eluent. Yield: 188 mg (26%) of **2** (isomer 2,8) and 143 mg (19%) of **2′** (isomer 2,3).

Characterization of ***2****.* ^{1}H 500 MHz NMR (δ in ppm in $CDCl_3$): 9.42 (d, 1H, P_9, J = 2.5 Hz); 8.34 (d, 1H, P_7, J = 2.5 Hz); 8.28 (d, 1H, P_4, J = 8.2 Hz); 7.85 (s, 2H, $T_{3'5'}$); 7.71 (d, 2H, P_a, J = 8.8 Hz); 7.55 (d, 1H, P_3, J = 8.2 Hz); 7.07 (d, 2H, P_b, J = 8.8 Hz); 6.95 (s, 2H, P_m); 3.89 (s, 3H, P_{OMe}); 2.35 (s, 3H, Me^p); 2.09 (s, 6H, Me°). HR FAB MS *m*/*z* (calc): 405.1971 (405.1967, $[M + H]^+$). Anal. Calcd for $C_{28}H_{24}N_2O$: C, 83.14; H, 5.98; N, 6.93, Found: C, 82.91; H, 6.10; N, 6.87.

Characterization of ***2′****.* ^{1}H 300 MHz NMR (δ in ppm in $CDCl_3$): 9.19 (dd, 1H, P_9, J = 4.3,1.7 Hz); 8.23 (dd, 1H, P_7, J = 8.1,1.9 Hz); 8.23 (s, 1H, P_4); 7.85 (d, 1H, P_5, J = 8.8 Hz); 7.79 (d, 1H, P_6, J = 8.8 Hz); 7.58 (dd, 1H, P_8, J = 8.1,4.3 Hz); 7.15 (d, 2H, P_a, J = 9.1 Hz); 6.78 (s, 2H, P_m); 6.77 (d, 2H, P_b, J = 9.1 Hz); 3.77 (s, 3H, P_{OMe}); 2.26 (s, 3H, Me^p); 1.93 (s, 6H, Me°).

3. In a 500 mL two-necked round-bottom flask 29.6 g (160 mmol) of 3-bromobenzaldehyde was dissolved in 250 mL of methanol. To the well-stirred solution were successively added 18 mL (160 mmol) of 2-acetylpyridine and a solution of 6.4 g of sodium hydroxide in 50 mL of water. The solution was stirred at room temperature for 15 min. The white precipitate was filtered, washed with water, and dissolved in dichloromethane. The organic phase was still washed once with water and evaporated to dryness to yield 28.2 g of chalcone **3** (61%). ^{1}H 500 MHz NMR (δ in ppm in $CDCl_3$): 8.75 (dq, 1H, $T_{6''}$, J = 4.8,0.9 Hz); 8.29 (d, 1H, $T_{4'}$, J = 16.1 Hz); 8.19 (dt, 1H, $T_{3''}$, J = 7.7,1.2 Hz); 7.88 (td, 1H, $T_{4''}$, J = 7.7,1.8 Hz); 7.88 (s, 1H, T_A); 7.84 (d, 1H, $T_{3'}$, J = 16.1 Hz); 7.62 (d, 1H, T_C, J = 7.7 Hz); 7.51 (m, 2H, $T_E + T_{5''}$); 7.28 (t, 1H, T_D, J = 7.9 Hz). Anal. Calcd for $C_{14}H_{10}BrNO$: C, 58.36; H, 3.50; N, 4.86. Found: C, 58.48; H, 3.72; N, 4.77.

6. In a 500 mL two-necked round-bottom flask was added 3.00 g (11.6 mmol) of 3-bromophenanthroline, 150 mL of toluene, and a stirring bar. The flask was put under argon, 669 mg (580 μmol, 5 mol %) of palladium tetrakis(triphenylphosphine) was added under argon, 60 mL (120 mmol) of a degassed 2 M aqueous sodium carbonate solution, and a degassed solution containing 2.12 g (13.9 mmol) of paramethoxyphenyl boronic acid in 100 mL of toluene and 15 mL of ethanol were successively cannulated into the reaction flask. The solution was degassed and refluxed under argon overnight. The solvents were evaporated, water was added and extracted with dichloromethane, and the organic phase was washed with water and evaporated to dryness. The crude product (5.05 g) was purified by chromatography on silica gel using dichloromethane/methanol mixtures as eluents to yield 3.01 g of phenanthroline **6** (91%). ^{1}H 300 MHz NMR (δ in ppm in $CDCl_3$): 9.33 (d, 1H, P_2, J = 2.4 Hz); 9.10 (dd, 1H, P_9, J = 4.4,1.8 Hz); 8.16 (d, 1H, P_4, J = 2.3 Hz); 8.08 (dd, 1H, P_7, J = 8.1,1.8 Hz); 7.63 (d, 2H, P_a, J = 3.3 Hz); 7.61−7.58 (m, 2H, $P_5 + P_6$); 7.49 (dd, 1H, P_8); 6.96 (d, 2H, P_b, J = 8.8 Hz); 3.77 (s, 3H, P_{OMe}). Anal. Calcd for $C_{19}H_{14}N_2O$: C, 79.70; H, 4.93; N, 9.78. Found: C, 79.54; H, 4.88; N, 9.66.

7. A 4.10 g (9.87 mmol) amount of 4′-(3-anisylphenyl)-2,2′;6′,2″-terpyridine and 2.59 g (9.9 mmol) triaquaruthenium trichloride was mixed in 500 mL of ethanol and refluxed under air for 1 h. The mixture was cooled to room temperature and filtered. The solid was washed twice with ethanol and dried to yield 5.84 g of a brown solid (95%). FAB MS *m*/*z* (calcd): 621.9 (622.0, $[M]^+$); 586.9 (587.0, $[M - Cl]^+$); 552.0 (552.0, $[M - 2Cl]^+$); 517.0 (517.1, $[M - 3Cl + H]^+$).

8_{th}^+. A 185 mg (297 μmol) amount of **7**, 40 mL of ethanol, and 53 mg (1.24 mmol) of lithium chloride were mixed in a two-necked 250 mL round-bottom flask. A 100 mg (248 μmol) amount of 8-anisyl-2-mesitylphenanthroline was dissolved in 40 mL of hot ethanol and added to the reaction mixture. A 20 mL amount of water and 2 mL of triethylamine were added; the reaction flask was put under argon and refluxed for 4 h. The violet complex precipitated after addition of 50 mL of KPF_6 and 30 mL of water at room temperature; the precipitate was filtered, washed with water, recovered with acetone, and dried. A minimum amount of acetone was added to dissolve the crude material, toluene was added until complete precipitation of the complex, and the remaining free phenanthroline, soluble in toluene, was removed by filtration. The

violet solid was recovered with acetone, dried, and purified by chromatography on silica gel using a 500:5:0.5 mixture of acetone, water, and KNO_3. Yield: 147 mg of analytically pure [$\mathbf{8_{th}}$][PF_6]. ^{1}H 500 MHz NMR (δ in ppm in $CDCl_3$): 10.88 (d, 1H, P_9); 8.83 (d, 1H, P_7); 8.32 (d, 1H, P_6, J = 8.9 Hz); 8.23 (d, 1H, P_4); 8.22 (d, 2H, $T_{33''}$); 8.11 (d, 1H, P_5, J = 8.9 Hz); 8.07 (s, 2H, $T_{3'5'}$); 7.97 (d, 2H, P_a, J = 8.0 Hz); 7.90 (s, 1H, T_A); 7.72 (m, 1H, T_E); 7.68 (d, 2H, T_a); 7.68 (td, 2H, $T_{44''}$); 7.67 (m, 1H, T_C); 7.57 (m, 1H, T_D); 7.44 (d, 2H, $T_{66''}$, J = 5.5 Hz); 7.10 (d, 2H, P_b, J = 8.0 Hz); 7.07 (m, 2H, $T_{55''}$); 7.02 (d, 2H, T_b, J = 8.0 Hz); 6.94 (d, 1H, P_3, J = 8.2 Hz); 6.37 (s, 2H, P_m); 3.87 (s, 3H, T_{MeO}); 3.85 (s, 3H, P_{MeO}); 1.86 (s, 3H, Me^p); 0.74 (s, 6H, Me^o). UV−vis (λ_{max} (ϵ in L mol^{-1} cm^{-1}) in acetone): 515 nm (17 100). ES MS *m/z* (calcd): 956.2305 (956.2305, [M − PF_6]$^+$).

$\mathbf{9_{th}}^{2+}$. A 131 mg (119 μmol) amount of [$\mathbf{8_{th}}$][PF_6] was dissolved in a mixture of 80 mL of acetonitrile and 20 mL of water. The solution was degassed and refluxed under argon for 2 days. Complete precipitation of the complex was obtained by adding enough KPF_6 at room temperature. The orange precipitate was filtered, washed with water, recovered with acetone, dried, and purified on silica gel using a 80:5:0.5 acetonitrile/water/KNO_3 mixture as the eluent. Yield: 112 mg (75%) of [$\mathbf{9_{th}}$][PF_6]$_2$. ^{1}H 300 MHz NMR (δ in ppm in CD_3CN): 9.94 (d, 1H, P_9); 9.11 (d, 1H, P_7); 8.54 (s, 2H, $T_{3'5'}$); 8.52 (m, 2H, $T_{33''}$); 8.49 (d, 1H, P_4); 8.44 (d, 1H, P_6, J = 8.9 Hz); 8.33 (s, 1H, T_A); 8.27 (d, 1H, P_5, J = 8.9 Hz); 8.06 (m, 5H, P_a + $T_{44''}$ + T_E); 7.86 (m, 3H, T_a + T_C); 7.81 (m, 1H, T_D); 7.61 (m, 2H, $T_{66''}$); 7.24 (m, 5H, P_3 + T_b + $T_{55''}$); 7.16 (d, 2H, P_b, J = 8.0 Hz); 6.53 (s, 2H, P_m); 3.91 (s, 3H, T_{MeO}); 3.90 (s, 3H, P_{MeO}); 2.08 (s, 3H, AN_{CH3}); 1.98 (s, 3H, Me^p); 0.86 (s, 6H, Me°). ES MS *m/z* (calcd): 481.136 (481.144, [M − 2PF_6]$^{2+}$); 460.62 (460.63, [M − CH_3CN − 2PF_6]$^{2+}$).

$\mathbf{9_{photo}}^{2+}$. A 50 mg (45 μmol) amount of [$\mathbf{8_{th}}$][PF_6] was dissolved in 4 mL of acetonitrile and 2 mL of water, put under argon, and white-light irradiated for 1 h at room temperature with a 1000 W xenon arc lamp filtered by a water filter. The resulting orange solution was transferred in 20 mL of KPF_6 upon which precipitation occurred. The solid was filtered, washed with water, recovered with acetone, and dried to yield 52 mg (100%) of the photochemical isomer [$\mathbf{9_{photo}}$][PF_6]$_2$. ^{1}H 300 MHz NMR (δ in ppm in CD_3CN): 8.92 (d, 1H, P_4, J = 8.3 Hz); 8.83 (s, 2H, $T_{3'5'}$); 8.58−8.55 (m, 3H, P_7 + $T_{33''}$); 8.41 (d, 1H, P_5, J = 8.8 Hz); 8.32 (t, 1H, T_A, J = 1.9 Hz); 8.21 (d, 1H, P_6, J = 8.8 Hz); 8.09−7.99 (m, 4H, T_E + P_3 + $T_{44''}$); 7.93−7.82 (m, 4H, T_C + P_9 + T_a); 7.80 (t, 1H, T_D, J = 7.9 Hz); 7.71−7.69 (m, 2H, $T_{66''}$); 7.31 (d, 2H, P_a, J = 8.9 Hz); 7.23 (m, 2H, $T_{55''}$); 7.12 (d, 2H, T_b, J = 8.8 Hz); 6.94 (s, 2H, P_m); 6.90 (d, 2H, P_b, J = 8.9 Hz); 3.88 (s, 3H, T_{MeO}); 3.74 (s, 3H, P_{MeO}); 2.24 (s, 3H, Me^p); 2.09 (s, 6H, Me^o). ES MS *m/z* (calcd): 460.6316 (460.6311, [M − 2PF_6 − CH_3CN]$^{2+}$); 1107.2534 (1107.2534, [M − PF_6]$^+$). UV−vis: (λ_{max} (ϵ in L mol^{-1} cm^{-1}) in acetone): 461 nm (12 500).

$\mathbf{10_{th}}^{2+}$. A 64 mg (51 μmol) amount of [$\mathbf{9_{th}}$][PF_6]$_2$ was dissolved in 5 mL of pyridine. The solution was degassed and refluxed under argon for 2 h. Precipitation was obtained by addition of KPF_6 at room temperature; the solid was filtered, washed with water, and recovered with acetone. Yield: 66 mg (100%) of [$\mathbf{10_{th}}$][PF_6]$_2$. ^{1}H 500 MHz NMR (δ in ppm in acetone-d_6): 9.28 (d, 1H, P_7, J = 1.8 Hz); 9.01 (d, 1H, P_9, J = 1.8 Hz); 8.94 (s, 2H, $T_{3'5'}$); 8.92 (d, 2H, $T_{33''}$, J = 8.1 Hz); 8.76 (d, 1H, P_4, J = 8.1 Hz); 8.62 (d, 1H, P_6, J = 8.8 Hz); 8.47 (d, 1H, P_5, J = 8.8 Hz); 8.37 (t, 1H, T_A, J = 1.8 Hz); 8.22 (td, 2H, $T_{44''}$, J = 7.7,1.5 Hz); 8.18 (m, 1H, T_E); 8.11 (m, 2H, $T_{66''}$); 7.90−7.86 (m, 2H, T_C + PY_p); 7.81−7.75 (m, 7H, PY_o + T_a + P_a + T_D); 7.51 (m, 2H, $T_{55''}$); 7.43 (d, 1H, P_3, J = 8.1 Hz); 7.32 (dd, 2H, PY_m); 7.12 (d, 2H, T_b, J = 8.8 Hz); 7.10 (d, 2H, P_b, J = 8.8 Hz); 6.63 (s, 2H, P_m); 3.90 (s, 3H, T_{MeO}); 3.86 (s, 3H, P_{MeO}); 2.03 (s, 3H, Me^p); 0.98 (s, 6H, Me°). UV−vis (λ_{max} (ϵ in L mol^{-1} cm^{-1}) in acetone): 485 nm (17 900). ES MS *m/z* (calcd): 500.157 (500.152, [M − 2PF_6]$^{2+}$); 1145.280 (1145.268, [M − PF_6]$^+$).

$\mathbf{10_{photo}}^{2+}$. *Thermal Preparation*. A 64 mg (51 μmol) amount of [$\mathbf{9_{photo}}$][PF_6]$_2$ was dissolved in 5 mL of pyridine. The solution was degassed and refluxed under argon for 2 h. Precipitation was obtained by addition of KPF_6 at room temperature; the solid was filtered, washed with water, and recovered with acetone. Yield: 65 mg (100%) of [$\mathbf{10_{photo}}$][PF_6]$_2$.

Photochemical Preparation. A 64 mg (51 μmol) amount of 9[PF_6]$_2$ (either thermal or photochemical isomer) was dissolved in 3 mL of pyridine. The solution was degassed and white-light irradiated for 1 h at room temperature with a 1000 W xenon arc lamp filtered by a water filter. Precipitation was obtained by addition of KPF_6; the solid was filtered, washed with water, and recovered with acetone. Yield: 66 mg (100%) of [$\mathbf{10_{photo}}$][PF_6]$_2$. ^{1}H 500 MHz NMR (δ in ppm in acetone-d_6): 9.14 (s, 2H, $T_{3'5'}$); 9.13 (d, 1H, P_4, J = 7.8 Hz); 8.90 (d, 2H, $T_{33''}$, J = 7.8 Hz); 8.78 (d, 1H, P_7, J = 2.0 Hz); 8.57 (d, 1H, P_5, J = 9.0 Hz); 8.38 (d, 1H, P_6, J = 8.4 Hz); 8.30 (m, 3H, T_A + $T_{66''}$); 8.19 (td, 2H, $T_{44''}$, J = 7.8,1.5 Hz); 8.07 (d, 1H, P_3, J = 8.4 Hz); 8.05 (m, 1H, T_E); 8.04 (d, 2H, P_9, J = 2.0 Hz); 7.84 (d, 1H, T_C, J = 8.5 Hz); 7.74 (d, 2H, T_a, J = 9.0 Hz); 7.70 (t, 1H, T_D, J = 7.8 Hz); 7.59 (t, 1H, PY_p, J = 7.8 Hz); 7.55 (m, 2H, $T_{55''}$); 7.31 (d, 2H, P_a, J = 8.4 Hz); 7.27 (d, 2H, PY_o, J = 5.4 Hz); 7.08 (d, 2H, T_b, J = 8.4 Hz); 6.87 (d, 2H, P_b, J = 8.4 Hz); 6.85 (t, 2H, PY_m, J = 7.2 Hz); 6.43 (s, 2H, P_m); 3.87 (s, 3H, T_{MeO}); 3.73 (s, 3H, P_{MeO}); 2.16 (s, 6H, Me°); 2.03 (s, 3H, Me^p). ES MS *m/z* (calcd): 500.146 (500.152, [M − 2PF_6]$^{2+}$); 1145.266 (1145.268, [M − PF_6]$^+$). UV−vis (λ_{max} (ϵ in L mol^{-1} cm^{-1}) in acetone): 482 nm (13 700).

$\mathbf{8_{photo}}^{+}$. A sample containing 5.0 mg (3.8 μmol) of [$\mathbf{10_{photo}}$][PF_6]$_2$ and 5.1 mg (31 μmol) of tetraethylammonium chloride in $C_2D_2Cl_4$ was prepared. The closed NMR tube was heated at 140 °C for 2 h in the dark and directly analyzed in the NMR spectrometer. Yield: 87% of [$\mathbf{8_{photo}}$][PF_6] and 13% of [$\mathbf{8_{th}}$][PF_6]. ^{1}H 500 MHz NMR (δ in ppm in $CDCl_3$): 8.70 (P_4); 8.34 ($T_{3'5'}$); 8.22 ($T_{33''}$); 8.22 (P_5); 8.20 (P_7); 8.09 (P_6); 7.93 (P_3); 7.93 (T_A); 7.72 (T_C); 7.70 (T_E); 7.65 ($T_{66''}$); 7.65 (T_D); 7.63 (P_9); 7.60 ($T_{44''}$); 7.13 (P_a); 7.08 ($T_{55''}$); 6.96 (T_a); 6.95 (T_a); 6.87 (P_b); 6.84 (P_m); 3.87 (T_{OMe}); 3.70 (P_{OMe}); 2.21 (Me^p); 2.16 (Me°). UV−vis (λ_{max} (ϵ in L mol^{-1} cm^{-1}) in acetone): 517 nm (11 000). ES MS *m/z* (calcd): 956.25 (956.23, [M − PF_6]$^+$).

$\mathbf{11_{th}}^{2+}$. A sample containing 5.0 mg (3.8 μmol) of [$\mathbf{10_{photo}}$][PF_6]$_2$ in CD_3SOCD_3 was prepared. The closed NMR tube was heated at 140 °C for 2 h in the dark, yielding a mixture of O-bonded and S-bonded thermal complexes. After waiting at room temperature for 8 h in the dark, the mixture evolved and the major product (S-bonded) remained almost alone. This complex was precipitated with KPF_6, washed with water, recovered with acetone, and dried, but purification on silica gel was impossible as it led to decomposition. Yield of [$\mathbf{11_{th}}$][PF_6]$_2$ > 95%. When [$\mathbf{11_{th}}$][PF_6]$_2$ was dissolved in acetonitrile, pyridine, or a dichloromethane solution of tetraethylammonium chloride and refluxed for 2 h under argon and in the dark it afforded complexes [$\mathbf{9_{th}}$][PF_6]$_2$, [$\mathbf{10_{th}}$][PF_6]$_2$, or [$\mathbf{8_{th}}$][PF_6], respectively. These complexes were purified on silica gel (acetone/water/KNO_3 80:5:0.5) with an overall yield (from the photochemical isomer) of ≈85%.

Characterization of [$\mathbf{11_{th}}$][PF_6]$_2$. ^{1}H 500 MHz NMR (δ in ppm in acetone-d_6): 11.04 (d, 1H, P_9, J = 2.1 Hz); 9.37 (d, 1H, P_7, J = 1.9 Hz); 9.06 (s, 2H, $T_{3'5'}$); 8.96 (d, 2H, $T_{33''}$, J = 7.6 Hz); 8.81 (d, 1H, P_4, J = 8.3 Hz); 8.60 (d, 1H, P_6, J = 8.8 Hz); 8.45−8.42 (m, 2H, P_5 + T_A); 8.33−8.23 (m, 3H, $T_{44''}$ + T_E); 8.18 (m, 2H, $T_{66''}$);

8.10 (d, 2H, T_a, $J = 9.1$ Hz); 7.96 (m, 1H, T_C); 7.85−7.81 (m, 3H, $T_D + P_a$); 7.55 (m, 2H, $T_{55''}$); 7.46 (d, 1H, P_3, $J = 8.1$ Hz); 7.26 (d, 2H, T_b, $J = 9.1$ Hz); 7.14 (d, 2H, P_b, $J = 9.1$ Hz); 6.62 (s, 2H, P_m); 3.94 (s, 3H, T_{MeO}); 3.90 (s, 3H, P_{MeO}); 1.17 (s, 6H, Me°). Me^p is hidden behind the residual solvent peak. ES MS *m*/*z* (calcd): 460.633 (460.631, $[M - CH_3SOCH_3 - 2PF_6]^{2+}$); 499.643 (499.638, $[M - 2PF_6]^{2+}$); 1144.244 (1144.241, $[M - PF_6]^+$). UV−vis (λ_{max} in DMSO): 437 nm (S-bonded); 490 nm (O-bonded).

12^{2+}. A 51 mg (39 μmol) amount of **10**$[PF_6]_2$ was weighed in a Schlenk flask, put under argon, dissolved with 3 mL of dry dichloromethane, and cooled to −78 °C. A 1.40 mL (1.40 mmol) amount of 1 M boron tribromide in DCM was added via a syringe at −78 °C. The mixture was stirred for 1.5 h at −78 °C and 1 h at 15 °C. A 2 mL amount of water and 2 mL of acetone were added, the solution was stirred at RT for 5 min, the organic solvents were evaporated, acetone was added, and the complex was precipitated with KPF_6. The solid was filtered, washed with water, and recovered with acetone. Yield of **12**$[PF_6]_2$: 50 mg (100%).

Characterization of ***12_{th}^{2+},2PF_6^-***. ^{1}H NMR 500 MHz (δ (ppm) in acetone-d_6): 9.26 (d, 1H, P_7, $J = 1.8$ Hz); 9.00 (d, 1H, P_9, $J = 1.8$ Hz); 8.96 (s, 2H, $T_{3'5'}$); 8.95 (d, 2H, $T_{33''}$, $J = 8.1$ Hz); 8.77 (d, 1H, P_4, $J = 8.1$ Hz); 8.62 (d, 1H, P_6, $J = 8.8$ Hz); 8.48 (d, 1H, P_5, $J = 8.8$ Hz); 8.33 (s, 1H, T_A); 8.24 (td, 2H, $T_{44''}$, $J = 7.7,1.5$ Hz); 8.15−8.13 (m, 3H, $T_E + T_{66''}$); 7.90 (td, 1H, PY_p); 7.85 (m, 1H, T_C); 7.79 (d, 2H, PY_o, $J = 5.1$ Hz); 7.75 (t, 1H, T_D); 7.70 (d, 2H, T_a, $J = 8.8$ Hz); 7.66 (d, 2H, P_a, $J = 8.4$ Hz); 7.52 (m, 2H, $T_{55''}$); 7.44 (d, 1H, P_3, $J = 8.1$ Hz); 7.33 (dd, 2H, PY_m); 7.03 (d, 2H, T_b, $J = 8.8$ Hz); 7.01 (d, 2H, P_b, $J = 8.8$ Hz); 6.63 (s, 2H, P_m); 2.03 (s, 3H, Me^p); 0.99 (s, 6H, Me°). UV−vis (λ_{max} (ϵ in L mol^{-1} cm^{-1}) in acetone): 485.5 nm (7390). ES MS *m*/*z* (calcd): 486.137 (486.136, $[M - 2PF_6]^{2+}$).

Characterization of ***12_{photo}^{2+},2PF_6^-***. ^{1}H NMR 500 MHz (δ (ppm) in CD_2Cl_2): 8.84 (d, 1H, P_4, $J = 7.8$ Hz); 8.55 (s, 2H, $T_{3'5'}$); 8.51 (d, 2H, $T_{33''}$, $J = 7.8$ Hz); 8.36 (d, 1H, P_7, $J = 2.0$ Hz); 8.35 (d, 1H, P_5, $J = 9.0$ Hz); 8.17 (d, 1H, P_6, $J = 8.4$ Hz); 8.07 (td, 2H, $T_{44''}$, $J = 7.8,1.5$ Hz); 8.02 (m, 1H, T_A, $J = 1.5$ Hz); 7.88 (d, 1H, P_3, $J = 8.4$ Hz); 7.84 (m, 3H, $T_E + T_{66''}$); 7.72 (m, 1H, T_C); 7.65−7.63 (m, 2H, $T_D + P_9$); 7.61 (d, 2H, T_a, $J = 9.0$ Hz); 7.42−7.38 (m, 3H, $T_{55''} + PY_p$); 7.09 (d, 2H, P_a, $J = 8.4$ Hz); 6.94 (d, 2H, T_b, $J = 8.4$ Hz); 6.92 (d, 2H, PY_o, $J = 5.4$ Hz); 6.81 (d, 2H, P_b, $J = 8.4$ Hz); 6.68 (dd, 2H, PY_m); 6.38 (s, 2H, P_m); 6.09 (s, 1H, OH_T); 5.63 (s, 1H, OH_P); 2.02 (s, 6H, Me°); 2.01 (s, 3H, Me^p). ES MS *m*/*z* (calcd): 486.16 (486.14, $[M - 2PF_6]^{2+}$). UV−vis (λ_{max} (ϵ in L mol^{-1} cm^{-1}) in acetone): 481 nm (11 000).

13^{2+}. A 53 mg (42 μmol) amount of **12**$[PF_6]_2$ (either thermal or photochemical isomer) was weighed in a 50 mL flask. A 79 mg (570 μmol) amount of potassium carbonate, 174 mg (794 μmol) of 10-bromoundec-1-ene, and 10 mL of dimethylformamide were added; the reaction flask was put under argon and stirred at 60 °C for 8 h. DMF was removed under vacuum, acetone was added, and the complex was precipitated by addition of KPF_6. The complex was filtered, washed with water, recovered with acetone, precipitated with diethyl ether, filtered, and washed with diethyl ether in order to remove the excess of the chain. The complex was recovered with acetone and dried. Yield of **13**$[PF_6]_2$: 65 mg (>99%).

Characterization of ***13_{th}^{2+},2PF_6^-***. ^{1}H NMR 500 MHz (δ (ppm) in acetone-d_6): 9.27 (d, 1H, P_7, $J = 1.8$ Hz); 9.00 (d, 1H, P_9, $J = 1.8$ Hz); 8.93 (s, 2H, $T_{3'5'}$); 8.92 (d, 2H, $T_{33''}$, $J = 8.1$ Hz); 8.75 (d, 1H, P_4, $J = 8.1$ Hz); 8.61 (d, 1H, P_6, $J = 8.8$ Hz); 8.47 (d, 1H, P_5, $J = 8.8$ Hz); 8.37 (s, 1H, T_A); 8.22 (td, 2H, $T_{44''}$, $J = 7.7,1.5$ Hz); 8.17 (m, 1H, T_E); 8.11 (m, 2H, $T_{66''}$); 7.90−7.86 (m, 2H, $T_C + PY_p$); 7.80−7.74 (m, 7H, $PY_o + T_a + P_a + T_D$); 7.51 (m, 2H, $T_{55''}$); 7.42 (d, 1H, P_3, $J = 8.1$ Hz); 7.32 (dd, 2H, PY_m); 7.12 (d, 2H, T_b, $J = 8.8$ Hz); 7.10 (d, 2H, P_b, $J = 8.8$ Hz); 6.63 (s, 2H, P_m); 5.87−5.76 (m, 2H, $\iota_T + \iota_P$); 5.02−4.89 (m, 4H, $\kappa_T + \kappa_P$); 4.11 (t, 2H, α_T, $J = 6.6$ Hz); 4.07 (t, 2H, α_P, $J = 6.6$ Hz); 2.05−2.03 (m, 4H, $\theta_T + \theta_P$); 2.03 (s, 3H, Me^p); 1.85−1.78 (m, 4H, $\beta_T + \beta_P$); 1.54−1.47 (m, 4H, $\gamma_T + \gamma_P$); 1.45−1.28 (m, $\delta_T\delta_P\epsilon_T\epsilon_P\zeta_T\zeta_P\eta_T\eta_P$); 0.98 (s, 6H, Me°). ES MS *m*/*z* (calcd): 624.29 (624.28, $[M - 2PF_6]^{2+}$). UV−vis (λ_{max} (ϵ in L mol^{-1} cm^{-1}) in acetone): 486 nm (15 900).

Characterization of ***13_{photo}^{2+},2PF_6^-***. ^{1}H NMR 500 MHz (δ (ppm) in acetone-d_6): 9.13 (s, 2H, $T_{3'5'}$); 9.12 (d, 1H, P_4, $J = 7.8$ Hz); 8.90 (d, 2H, $T_{33''}$, $J = 7.8$ Hz); 8.77 (d, 1H, P_7, $J = 2.0$ Hz); 8.57 (d, 1H, P_5, $J = 9.0$ Hz); 8.37 (d, 1H, P_6, $J = 8.4$ Hz); 8.30−8.28 (m, 3H, $T_A + T_{66''}$); 8.19 (td, 2H, $T_{44''}$, $J = 7.8,1.5$ Hz); 8.07 (d, 1H, P_3, $J = 8.4$ Hz); 8.03 (m, 1H, T_E); 8.02 (d, 2H, P_9, $J = 2.0$ Hz); 7.84 (d, 1H, T_C, $J = 8.5$ Hz); 7.73 (d, 2H, T_a, $J = 9.0$ Hz); 7.70 (t, 1T, T_D, $J = 7.8$ Hz); 7.59 (t, 1H, PY_p, $J = 7.8$ Hz); 7.55 (m, 2H, $T_{55''}$); 7.29 (d, 2H, P_a, $J = 8.4$ Hz); 7.27 (d, 2H, PY_o, $J = 5.4$ Hz); 7.08 (d, 2H, T_b, $J = 8.4$ Hz); 6.86 (d, 2H, P_b, $J = 8.4$ Hz); 6.85 (t, 2H, PY_m, $J = 7.2$ Hz); 6.43 (s, 2H, P_m); 5.86−5.74 (m, 2H, $\iota_P + \iota_T$); 5.02−4.87 (m, 4H, $\kappa_P + \kappa_T$); 4.08 (t, 2H, α_T, $J = 6.6$ Hz); 3.92 (t, 2H, α_P, $J = 6.4$ Hz); 2.16 (s, 6H, Me°); 2.03 (s, 3H, Me^p); 2.03−1.95 (m, 4H, $\theta_T + \theta_P$); 1.82 (q, 2H, β_T, $J = 6.6$ Hz); 1.69 (q, 2H, β_P, $J = 6.6$ Hz); 1.52 (q, 2H, γ_T, $J = 7.3$ Hz); 1.44−1.26 (m, 18H, $\gamma_P\epsilon_T\epsilon_P\delta_T\delta_P\zeta_T\zeta_P\eta_T\eta_P$). ES MS *m*/*z* (calcd): 624.2772 (624.2772, $[M - 2PF_6]^{2+}$). UV−vis (λ_{max} (ϵ in L mol^{-1} cm^{-1}) in acetone): 481 nm (11 000).

14_{th}^{2+}. A 35 mg (28 μmol) amount of $[\mathbf{12_{th}}][PF_6]_2$ was weighed in a 50 mL flask. A 38 mg (280 μmol) amount of potassium carbonate, 140 mg (560 μmol) of (2(2-bromoethoxy)ethoxy)ethyl allyl ether, and 10 mL of dimethylformamide were added; the reaction flask was put under argon and stirred at 60 °C for 8 h. DMF was removed under vacuum, acetone was added, and the complex was precipitated by addition of KPF_6. The complex was filtered, washed with water, recovered with acetone, and purified over 200 mL of fine silica gel (eluent acetone/water/KNO_3 100:5:0.1). Yield: 39 mg (87%). ^{1}H NMR 500 MHz (δ (ppm) in acetone-d_6): 9.30 (d, 1H, P_7, $J = 1.8$ Hz); 9.07 (d, 1H, P_9, $J = 1.8$ Hz); 8.96 (s, 2H, $T_{3'5'}$); 8.94 (d, 2H, $T_{33''}$, $J = 8.1$ Hz); 8.77 (d, 1H, P_4, $J = 8.1$ Hz); 8.62 (d, 1H, P_6, $J = 8.8$ Hz); 8.48 (d, 1H, P_5, $J = 8.8$ Hz); 8.37 (s, 1H, T_A); 8.24 (td, 2H, $T_{44''}$, $J = 7.7,1.5$ Hz); 8.17 (m, 1H, T_E); 8.13 (m, 2H, $T_{66''}$); 7.90−7.87 (m, 2H, $T_D + PY_p$); 7.83 (m, 1H, T_C); 7.80−7.74 (m, 6H, $PY_o + T_a + P_a$); 7.51 (m, 2H, $T_{55''}$); 7.44 (d, 1H, P_3, $J = 8.1$ Hz); 7.32 (dd, 2H, PY_m); 7.14 (d, 2H, T_b, $J = 8.8$ Hz); 7.12 (d, 2H, P_b, $J = 8.8$ Hz); 6.63 (s, 2H, P_m); 5.94−5.84 (m, 2H, $\theta_T + \theta_P$); 5.28−5.22 (m, 2H, *cis*-$\iota_T + \iota_P$); 5.12−5.08 (m, 2H, *trans*- $\iota_T + \iota_P$); 4.25−4.20 (m, 4H, $\alpha_T + \alpha_P$); 4.00−3.96 (m, 4H, $\eta_T + \eta_P$); 3.89−3.83 (m, 4H, $\beta_T + \beta_P$); 3.71−3.55 (m, 16H, $\gamma_T\gamma_P\delta_T\delta_P\epsilon_T\epsilon_P\zeta_T\zeta_P$); 2.04 (s, 3H, Me^p); 0.99 (s, 6H, Me°). ES MS *m*/*z* (calcd): 658.246 (658.247, $[M\text{-}2PF_6]^{2+}$). UV−vis (λ_{max} (ϵ in L mol^{-1} cm^{-1}) in acetone): 486 nm (12 000).

14_{photo}^{2+}. A 50.4 mg (40 μmol) amount of $[\mathbf{12_{photo}}][PF_6]_2$, 63 mg (456 μmol) of K_2CO_3, and 107 mg (422 mmol) of (2(2-bromoethoxy)ethoxy)ethyl allyl ether were weighed in a flask. An 8 mL amount of dimethylformamide was added; the reaction mixture was put under argon and stirred at 60 °C for 8 h. DMF was removed by high vacuum; acetone was added followed by KPF_6 until precipitation occurred. The complex was filtered, washed with water, recovered with acetone, dried, and purified over silica gel (eluent acetone/water/KNO_3 100:5:0.1). The main fraction was precipitated by KPF_6, washed with water, recovered with acetone, and dried to afford 58.3 mg of precursor $[\mathbf{14_{photo}}][PF_6]_2$ (91%). ^{1}H NMR 500 MHz (δ (ppm) in acetone-d_6): 9.15 (s, 2H, $T_{3'5'}$); 9.13 (d, 1H, P_4, $J = 8.0$ Hz); 8.91 (d, 2H, $T_{33''}$, $J = 8.1$ Hz); 8.79 (d,

1H, P_9, $J = 1.8$ Hz); 8.58 (d, 1H, P_5, $J = 8.8$ Hz); 8.39 (d, 1H, P_6, $J = 8.8$ Hz); 8.31 (m, 2H, $T_{66''}$); 8.29 (t, 1H, T_A, $J = 1.8$ Hz); 8.20 (td, 2H, $T_{44''}$, $J = 7.7,1.5$ Hz); 8.09 (d, 1H, P_3, $J = 8.1$ Hz); 8.04 (d, 1H, P_9, $J = 2.0$ Hz); 8.03 (m, 1H, T_E); 7.86 (m, 1H, T_C); 7.74 (d, 2H, T_a, $J = 8.9$ Hz); 7.71 (m, 1H, T_D); 7.59 (tt, 1H, PY_p, $J = 7.7,1.5$ Hz); 7.55 (m, 2H, $T_{55''}$); 7.31 (d, 2H, P_a, $J = 8.9$ Hz); 7.28 (m, 2H, PY_o); 7.11 (d, 2H, T_b, $J = 8.9$ Hz); 6.89 (d, 2H, P_b, $J = 8.8$ Hz); 6.85 (m, 2H, PY_m); 6.43 (s, 2H, P_m); 5.93−5.80 (m, 2H, $\theta_T + q_P$); 5.26 (ddd, 1H, *trans*-ι_T, $J = 17.3,3.8,1.7$ Hz); 5.20 (ddd, 1H, *trans*-ι_P, $J = 17.3,3.8,1.7$ Hz); 5.10 (ddd, 1H, *cis*-ι_T, $J = 10.5,2.1,1.5$ Hz); 5.05 (ddd, 1H, *cis*-ι_P, $J = 10.5,2.1,1.5$ Hz); 4.22 (m, 2H, α_T); 4.06 (m, 2H, α_P); 3.99 (m, 2H, η_T); 3.93 (m, 2H, η_P); 3.87 (m, 2H, β_T); 3.75 (m, 2H, β_P); 3.69 (m, 2H, γ_T); 3.64 (m, 2H, δ_T); 3.62 (m, 2H, ϵ_T); 3.59 (m, 2H, γ_P); 3.57 (m, 2H, ζ_T); 3.56 (m, 2H, δ_P); 3.54 (m, 2H, ϵ_P); 3.51 (m, 2H, ζ_P); 2.16 (s, 6H, Me°); 2.03 (s, 3H, Me^p). ES MS *m*/*z* (calcd): 658.2470 (658.2468, $[M - 2PF_6]^{2+}$); 1461.451 (1461.458, $[M - PF_6]^+$). UV−vis (λ_{max} (ϵ in L mol^{-1} cm^{-1}) in acetone): 481.5 nm (12 800).

15_{th}^{2+}. A 17 mg amount of $[\mathbf{13}_{th}][PF_6]_2$ and 13 mg of Grubbs' first-generation catalyst were dissolved in dichloromethane and stirred under argon in the dark for 7 days. Acetone was added along with aqueous potassium hexafluorophosphate, and removal of the organic solvents led to precipitation of the complex. The solid was filtered, washed with water, and recovered with acetone. Chromatography over silica gel (acetone/water/KNO_3 100:5:0.1 to 60:5:1) was undertaken in order to separate, in this order, the remaining starting material, the monomer $[\mathbf{15}_{th}][PF_6]_2$ (3.6 mg, 21%), and the dimer (4.3 mg, 25% yield). ES MS *m*/*z* (calcd): for the monomer 610.31 (610.26, $[M - 2PF_6]^{2+}$); for the dimer 610.31 (610.26, $[M - 4PF_6]^{4+}$); 862.06 (862.00, $[M - 3PF_6]^{3+}$); 1365.6 (1365.5, $[M - 2PF_6]^{2+}$).

16_{th}^{2+}. A 31 mg (19 μmol) amount of $[\mathbf{14}_{th}][PF_6]_2$ and 13 mg (16 μmol) of Grubbs' first-generation catalyst were weighed in a flask and put under argon. A 100 mL amount of dry dichloromethane was added in the dark, and the solution was stirred for 5 days and flushed with argon regularly. The DCM was removed under vacuum, acetone was added, and the complex was precipitated with KPF_6, filtered, washed with water, recovered with acetone, and put on 200 mL of fine silica gel for purification (eluent, acetone/water/KNO_3 80:5:0.3). The monomer was the less polar fraction and the dimer the most polar. Yield: 8.1 mg of the monomer $[\mathbf{16}_{th}][PF_6]_2$ (26%) and 8.7 mg for the corresponding dimer (28%). ^{1}H NMR 500 MHz (δ (ppm) in acetone-d_6): 9.26 (d, 1H, P_7, $J = 1.8$ Hz); 8.91 (d, 2H, $T_{33''}$, $J = 8.1$ Hz); 8.84 (s, 2H, $T_{3'5'}$); 8.81 (d, 1H, P_9, $J = 1.8$ Hz); 8.80 (d, 1H, P_4, $J = 8.1$ Hz); 8.63 (d, 1H, P_6, $J = 8.8$ Hz); 8.50 (d, 1H, P_5, $J = 8.8$ Hz); 8.24 (td, 2H, $T_{44''}$, $J = 7.7,1.5$ Hz); 8.19 (m, 1H, T_E); 8.08 (m, 2H, $T_{66''}$); 7.95 (s, 1H, T_A); 7.89−7.85 (m, 2H, $T_C + PY_p$); 7.78 (m, 1H, T_D); 7.73 (d, 2H, PY_o, $J = 5.5$ Hz); 7.68 (d, 2H, T_a, $J = 9.0$ Hz); 7.66 (d, 2H, P_a, $J = 9.0$ Hz); 7.53−7.49 (m, 3H, $P_3 + T_{55''}$); 7.29 (dd, 2H, PY_m); 7.14 (d, 2H, T_b, $J = 8.8$ Hz); 7.13 (d, 2H, P_b, $J = 8.8$ Hz); 6.67 (s, 2H, P_m); 5.66 (m, 2H, $\theta_T + \theta_P$); 4.28 (m, 4H, $\alpha_T + \alpha_P$); 3.87 (m, 4H, $\eta_T + \eta_P$); 3.80,3.76 (m, 2 × 2H, β_T and β_P); 3.62 (m, 2H, γ_T); 3.56 (m, 2H, γ_P); 3.55 (m, 2H, δ_T); 3.50 (m, 2H, δ_P); 3.49 (m, 2H, ϵ_T); 3.46 (m, 2H, ϵ_P); 3.46 (m, 2H, ζ_T); 3.43 (m, 2H, ζ_P); 2.14 (s, 3H, Me^p); 0.95 (s, 6H, Me°). ES MS *m*/*z* (calcd): 644.2317 (644.2311, $[M - 2PF_6]^{2+}$); 1433.44 (1433.43, $[M - PF_6]^+$).

15_{photo}^{2+}. A 157 mg (102 μmol) amount of $[\mathbf{13}_{photo}][PF_6]_2$ and 35 mg (42 μmol) of Grubbs' first-generation catalyst were weighed in a 100 mL flask and put under argon. A 150 mL amount of dry dichloromethane was cannulated, and the solution was stirred in the dark at room temperature for 36 h. During the course of the reaction the solution was flushed three times with argon in order to remove ethylene. The DCM was evaporated, acetone was added, and the complex was precipitated with KPF_6, filtered, washed with water, recovered with acetone, and purified over 200 mL of fine silica gel (eluent, acetone/water/KNO_3 80:5:0.5). Yield: 115 mg of $[\mathbf{15}_{photo}][PF_6]_2$ (71%). ^{1}H NMR 500 MHz (δ (ppm) in acetone-d_6): 9.13 (s, 2H, $T_{3'5'}$); 9.12 (d, 1H, P_4, $J = 7.8$ Hz); 8.90 (d, 2H, $T_{33''}$, $J = 7.8$ Hz); 8.77 (d, 1H, P_7, $J = 2.0$ Hz); 8.57 (d, 1H, P_5, $J = 9.0$ Hz); 8.37 (d, 1H, P_6, $J = 8.4$ Hz); 8.30−8.28 (m, 3H, $T_A + T_{66''}$); 8.19 (td, 2H, $T_{44''}$, $J = 7.8,1.5$ Hz); 8.07 (d, 1H, P_3, $J = 8.4$ Hz); 8.03 (m, 1H, T_E); 8.02 (d, 2H, P_9, $J = 2.0$ Hz); 7.84 (d, 1H, T_C, $J = 8.5$ Hz); 7.73 (d, 2H, T_a, $J = 9.0$ Hz); 7.70 (t, 1H, T_D, $J = 7.8$ Hz); 7.59 (t, 1H, PY_p, $J = 7.8$ Hz); 7.55 (m, 2H, $T_{55''}$); 7.29 (d, 2H, P_a, $J = 8.4$ Hz); 7.27 (d, 2H, PY_o, $J = 5.4$ Hz); 7.08 (d, 2H, T_b, $J = 8.4$ Hz); 6.86 (d, 2H, P_b, $J = 8.4$ Hz); 6.85 (t, 2H, PY_m, $J = 7.2$ Hz); 6.43 (s, 2H, P_m); 5.86−5.74 (m, 2H, $\iota_P + \iota_T$); 5.02−4.87 (m, 4H, $\kappa_P + \kappa_T$); 4.08 (t, 2H, α_T, $J = 6.6$ Hz); 3.92 (t, 2H, α_P, $J = 6.4$ Hz); 2.16 (s, 6H, Me°); 2.03 (s, 3H, Me^p). UV−vis (λ_{max} (ϵ in L mol^{-1} cm^{-1}) in acetone): 481 nm. ES MS *m*/*z* (calcd): 610.27 (610.26, $[M - 2PF_6]^{2+}$); 1365.51 (1365.49, $[M - PF_6]^+$).

16_{photo}^{2+}. A 50 mg (31 μmol) amount of $[\mathbf{14}_{photo}][PF_6]_2$ and 10 mg (12 μmol) of Grubbs' first-generation catalyst were weighed in a 100 mL flask and put under argon. A 50 mL amount of dry dichloromethane was cannulated, and the solution was stirred in the dark at room temperature for 60 h. During the course of the reaction the solution was flushed three times with argon in order to remove ethylene. The DCM was evaporated, acetone was added, and the complex was precipitated with KPF_6, filtered, washed with water, recovered with acetone, and purified over 180 mL of silica gel (eluent, acetone/water/KNO_3 100:5:0.1 to 80:5:0.5). Yield: 41 mg of $[\mathbf{16}_{photo}][PF_6]_2$ (83%). ^{1}H NMR 500 MHz (δ (ppm) in acetone-d_6): 9.15 (s, 2H, $T_{3'5'}$); 9.13 (d, 1H, P_4, $J = 7.8$ Hz); 8.91 (d, 2H, $T_{33''}$, $J = 7.8$ Hz); 8.78 (d, 1H, P_7, $J = 2.0$ Hz); 8.58 (d, 1H, P_5, $J = 9.0$ Hz); 8.38 (m, 2H, $T_A + P_6$); 8.31 (d, 2H, $T_{66''}$, $J = 5.5$ Hz); 8.20 (td, 2H, $T_{44''}$, $J = 7.8,1.5$ Hz); 8.09 (d, 1H, P_3, $J = 8.4$ Hz); 7.98 (d, 2H, P_9, $J = 2.0$ Hz); 7.97 (m, 1H, T_E); 7.85 (d, 1H, T_C, $J = 8.5$ Hz); 7.77 (d, 2H, T_a, $J = 9.0$ Hz); 7.69 (m, 1H, T_D); 7.60 (t, 1H, PY_p); 7.55 (m, 2H, $T_{55''}$); 7.30 (d, 2H, P_a, $J = 8.4$ Hz); 7.28 (d, 2H, PY_o, $J = 5.4$ Hz); 7.13 (d, 2H, T_b, $J = 8.4$ Hz); 6.87 (d, 2H, P_b, $J = 8.4$ Hz); 6.86 (m, 2H, PY_m); 6.44 (s, 2H, P_m); 5.76 (m, 69% of 2H, $\theta_P + \theta_T$); 5.62 (m, 31% of 2H, $\theta_P + \theta_T$); 4.23 (m, 2H, α_T); 4.03 (m, 2H, α_P); 3.99 (m, 2H, η_T); 3.93 (m, 2H, η_P); 3.88 (m, 2H, β_T); 3.72 (m, 2H, β_P); 3.69 (m, 2H, γ_T); 3.63 (m, 2H, δ_T); 3.62 (m, 2H, γ_P); 3.57 (m, 2H, δ_P); 3.56−3.52 (m, 6H, $\epsilon_T + \zeta_T + \epsilon_P$); 3.49 (m, 2H, ζ_P); 2.17 (s, 6H, Me°); 2.03 (s, 3H, Me^p). ES MS *m*/*z* (calcd): 644.22 (644.23, $[M - 2PF_6]^{2+}$); 1433.39 (1433.43, $[M - PF_6]^+$). UV−vis (λ_{max} (ϵ in L mol^{-1} cm^{-1}) in acetone): 479.5 nm (13 200).

17_{th}^{2+}. A 16 mg (11 μmol) amount of $[\mathbf{17}_{photo}][PF_6]_2$ was dissolved in 4 mL of distilled DMSO, put under argon, and heated in the dark at 140 °C for 2 h. The complex was precipitated with KPF_6, filtered, washed with water, recovered with acetone, and dried. A 4 mL amount of pyridine was added; the solution was flushed with argon and refluxed for 2 h under argon. KPF_6 was added until complete precipitation; the solid was filtered, washed with water, recovered with acetone, and dried. Column chromatography on 80 mL of silica gel (eluent, acetone/water/KNO_3 80:5:0.5) yielded 13 mg of $[\mathbf{17}_{th}][PF_6]_2$ (85%). ^{1}H NMR 500 MHz (δ (ppm) in CD_2Cl_2): 8.90 (d, 1H, P_7, $J = 1.8$ Hz); 8.49 (d, 1H, P_4, $J = 8.1$ Hz); 8.44 (d, 3H, $P_6 + T_{33''}$); 8.40 (d, 1H, P_9, $J = 1.8$ Hz); 8.28 (d, 1H, P_5, $J = 8.8$ Hz); 8.21 (s, 2H, $T_{3'5'}$); 8.10 (td, 2H, $T_{44''}$, $J = 7.7,1.5$ Hz); 7.88 (m, 1H, T_E); 7.79 (m, 1H, T_C); 7.74 (m, 1H, T_D); 7.67−7.63 (m, 6H, $T_a + T_{66''} + T_A + PY_p$); 7.50 (d, 2H, P_a,

J = 8.8 Hz); 7.42 (m, 2H, $T_{55''}$); 7.32 (d, 2H, PY_o, J = 5 Hz); 7.29 (d, 1H, P_3, J = 8.1 Hz); 7.18 (m, 2H, PY_m); 7.01 (d, 2H, T_b, J = 8.8 Hz); 6.99 (d, 2H, P_b, J = 8.8 Hz); 6.59 (s, 2H, P_m); 4.09 (t, 2H, α_T, J = 6.6 Hz); 4.07 (t, 2H, α_P, J = 7.0 Hz); 2.17 (s, 3H, Me^p); 1.73 (m, 4H, $\beta_T + \beta_P$); 1.37 (4H, $\gamma_T + \gamma_P$); 1.34−1.18 (m, 24H, $\delta_T - \iota_T + \delta_P - \iota_P$); 0.83 (s, 6H, Me°). HR ES MS *m*/*z* (calcd): 611.2676 (611.2688, $[M - 2PF_6]^{2+}$).

17_{photo}^{2+}. A 50 mg (33 mol) amount of the unsaturated macrocycle [**15_{photo}**][PF_6]$_2$ and 14 mg of 10% palladium black on carbon were weighed in a flask and dissolved with 8 mL of dichloromethane and 5 mL of ethanol. The solution was saturated with hydrogen by 5 min of bubbling and stirred under a hydrogen atmosphere in the dark for 24 h. The reaction mixture was filtered on celite to remove the catalyst, and solvents were evaporated. Yield: 50 mg of [**17_{photo}**][PF_6]$_2$ (100%). ^{1}H NMR 500 MHz (δ (ppm) in CD_2Cl_2): 8.85 (d, 1H, P_4, J = 7.8 Hz); 8.57 (s, 2H, $T_{3'5'}$); 8.52 (d, 2H, $T_{33''}$, J = 7.8 Hz); 8.41 (d, 1H, P_7, J = 2.0 Hz); 8.37 (d, 1H, P_5, J = 9.0 Hz); 8.19 (d, 1H, P_6, J = 8.4 Hz); 8.14 (s, 1H, T_A); 8.10 (td, 2H, $T_{44''}$, J = 7.8,1.5 Hz); 7.89 (d, 1H, P_3, J = 8.4 Hz); 7.85 (m, 2H, $T_{66''}$); 7.81−7.79 (m, 2H, $T_C + T_E$); 7.73 (d, 2H, T_a, J = 9.0 Hz); 7.67 (t, 1H, T_D, J = 7.8 Hz); 7.65 (d, 2H, P_9, J = 2.0 Hz); 7.43 (m, 2H, $T_{55''}$); 7.40 (t, 1H, PY_p, J = 7.8 Hz); 7.16 (d, 2H, P_a, J = 8.4 Hz); 7.06 (d, 2H, T_b, J = 8.4 Hz); 6.92 (d, 2H, PY_o, J = 5.4 Hz); 6.88 (d, 2H, P_b, J = 8.4 Hz); 6.69 (t, 2H, PY_m, J = 7.2 Hz); 6.39 (s, 2H, P_m); 4.06 (t, 2H, α_T, J = 6.6 Hz); 3.86 (t, 2H, α_P, J = 6.4 Hz); 2.03 (s, 6H, Me°); 2.02 (s, 3H, Me^p); 1.82 (q, 2H, β_T, J = 6.6 Hz); 1.70 (q, 2H, β_P, J = 6.6 Hz); 1.55−1.47 (m, 2H, γ_T); 1.42−1.23 (m, 26H, $\gamma_P - \iota_P + \delta_T - \iota_T$). ES MS *m*/*z* (calcd): 1367.3 (1367.5, $[M - PF_6]^+$). UV−vis (λ_{max} (ϵ in L mol^{-1} cm^{-1}) in acetone): 481 nm (10 700).

18_{th}^{2+}. A 8 mg (5 μmol) amount of [**16_{th}**][PF_6]$_2$ was weighed along with 7 mg of 10% palladium black on carbon. A 2 mL amount of ethanol and 4 mL of dichloromethane were added; the mixture was saturated with hydrogen in 5 min of bubbling and stirred for 24 h at room temperature in the dark under a 1 atm hydrogen pressure. The catalyst was removed by filtration of the reaction mixture on celite, the solvents were evaporated, and the product was purified by chromatography on 90 mL of fine silica gel (eluent, acetone/water/KNO_3 80:5:0.5). The main fraction contained 7 mg (87%) of the reduced macrocycle [**18_{th}**][PF_6]$_2$. ^{1}H NMR 500 MHz (δ (ppm) in CD_2Cl_2): 8.91 (d, 1H, P_7, J = 1.8 Hz); 8.49 (d, 1H, J = 8.1 Hz); 8.46−8.43 (m, 4H, $T_{33''} + P_6 + P_4$); 8.37 (d, 1H, P_9, J = 1.8 Hz); 8.28 (d, 1H, P_5, J = 8.8 Hz); 8.23 (s, 2H, $T_{3'5'}$); 8.11 (t, 2H, $T_{44''}$, J = 7.7 Hz); 7.92 (m, 1H, T_E); 7.80 (m, 1H, T_C); 7.76 (m, 1H, T_D); 7.72 (s, 1H, T_A); 7.70 (m, 1H, PY_p); 7.65 (m, 4H, $T_a + T_{66''}$); 7.51 (d, 2H, P_a, J = 9.0 Hz); 7.43 (m, 2H, $T_{55''}$); 7.28 (m, 3H, $P_3 + PY_o$); 7.17 (m, 2H, PY_m); 7.08 (d, 2H, T_b, J = 8.8 Hz); 7.07 (d, 2H, P_b, J = 8.8 Hz); 6.59 (s, 2H, P_m); 4.23 (m, 4H, $\alpha_T + \alpha_P$); 3.78 (m, 4H, $\beta_T + \beta_P$); 3.63−3.46 (m, 20H, $\gamma_T + \gamma_P + \delta_T + \delta_P + \epsilon_T + \epsilon_P + \zeta_T + \zeta_P$); 3.36 (m, 4H, $\eta_T + \eta_P$); 2.16 (s, 3H, Me^p); 1.53 (m, 4H, $\theta_T + \theta_P$); 0.84 (s, 6H, Me°). HD ES MS *m*/*z* (calcd): 645.236 (645.238, $[M - 2PF_6]^{2+}$).

18_{photo}^{2+}. A 6 mg amount of [**18_{th}**][PF_6]$_2$ was dissolved in 2 mL of pyridine and irradiated for 1 h at room temperature with a Xenon 1000 W arc lamp filtered by a water filter. The complex was precipitated by addition of KPF_6, filtered, washed with water, recovered with acetone, and dried. Yield of [**18_{photo}**][PF_6]$_2$: 100%. ^{1}H NMR 500 MHz (δ (ppm) in CD_2Cl_2): 8.85 (d, 1H, P_4, J = 7.8 Hz); 8.57 (s, 2H, $T_{3'5'}$); 8.51 (d, 2H, $T_{33''}$, J = 7.8 Hz); 8.42 (d, 1H, P_7, J = 2.0 Hz); 8.37 (d, 1H, P_5, J = 9.0 Hz); 8.19 (d, 1H, P_6, J = 8.4 Hz); 8.10 (td, 3H, $T_{44''} + T_A$); 7.90 (d, 1H, P_3, J = 8.4 Hz); 7.86 (m, 2H, $T_{66''}$); 7.82−7.79 (m, 2H, $T_C + T_E$); 7.71 (d, 2H, T_a, J = 9.0 Hz); 7.68 (t, 1H, T_D, J = 7.8 Hz); 7.63 (d, 2H, P_9, J = 2.0 Hz); 7.45−7.41 (m, 3H, $T_{55''} + PY_p$); 7.16 (d, 2H, P_a, J = 8.4 Hz); 7.09 (d, 2H, T_b, J = 8.4 Hz); 6.93−6.90 (d, 4H, $PY_o + P_b$); 6.70 (t, 2H, PY_m, J = 7.2 Hz); 6.39 (s, 2H, P_m); 4.21 (m, 2H, α_T); 4.02 (m, 2H, α_P); 3.87 (m, 2H, β_T); 3.74 (m, 2H, β_P); 3.71−3.69 (m, 2H, γ_T); 3.65−3.63 (m, 2H, δ_T); 3.61−3.58 (m, 4H, $\gamma_P + \epsilon_T$); 3.57−3.52 (m, 6H, $\delta_P + \zeta_T + \epsilon_P$); 3.50 (m, 2H, ζ_P); 3.43 (m, 2H, η_T); 3.42 (m, 2H, η_P); 2.03 (s, 6H, Me°); 2.02 (s, 3H, Me^p); 1.60 (m, 4H, $\theta_T + \theta_P$). UV−vis (λ_{max} (ϵ in L mol^{-1} cm^{-1}) in acetone): 479.5 nm (11 600). HD ES MS *m*/*z* (calcd): 645.2391 (645.2389, $[M - 2PF_6]^{2+}$).

19_{photo}^{2+}. A 3.6 mg (2.4 μmol) amount of [**17_{photo}**][PF_6]$_2$ was dissolved in 1 mL of 3,5-dimethylpyridine, put under argon, and heated in the dark at 140 °C for 2 h. The complex was precipitated with heptane, filtered, washed with heptane, recovered with acetone, and dried to give quantitatively [**19_{photo}**][PF_6]$_2$. ^{1}H NMR 300 MHz (δ (ppm) in acetone-d_6): 9.15 (s, 2H, $T_{3'5'}$); 9.13 (d, 1H, P_4); 8.92 (d, 2H, $T_{33''}$); 8.79 (d, 1H, P_7); 8.59 (d, 1H, P_5); 8.39 (d, 1H, P_6); 8.37 (s, 1H, T_A); 8.31 (m, 2H, $T_{66''}$); 8.22 (td, 2H, $T_{44''}$); 8.07 (d, 1H, P_3); 8.03 (d, 2H, P_9); 7.97 (m, 1H, T_C); 7.86 (m, 1H, T_E); 7.78 (d, 2H, T_a); 7.69 (m, 1H, T_D); 7.56 (m, 2H, $T_{55''}$); 7.31 (d, 2H, P_a); 7.22 (s, 1H, L_p); 7.10 (d, 2H, T_b); 6.85 (d, 2H, P_b); 6.74 (s, 2H, L_o); 6.53 (s, 2H, P_m); 4.11 (t, 2H, α_T); 3.89 (t, 2H, α_P); 2.18 (s, 6H, Me°); 2.02 (s, 3H, Me^p); 1.84 (s, 6H, L_{CH3}); 1.68 (m, 2H, β_T); 1.52 (m, 2H, β_P); 1.45−1.23 (m, 28H, $\gamma_P - \iota_P + \gamma_T - \iota_T$).

20_{photo}^{2+}. A 3.6 mg (2.4 μmol) amount of [**17_{photo}**][PF_6]$_2$ was dissolved in 1 mL of benzonitrile, put under argon, and heated in the dark at 140 °C for 2 h. The complex was precipitated with heptane, filtered, washed with heptane, recovered with acetone, and dried to give quantitatively [**20_{photo}**][PF_6]$_2$. ^{1}H NMR 300 MHz (δ (ppm) in CD_2Cl_2): 8.86 (d, 1H, P_4); 8.71 (s, 2H, $T_{3'5'}$); 8.58 (d, 2H, $T_{33''}$); 8.45 (d, 1H, P_7); 8.37 (d, 1H, P_5); 8.20 (d, 1H, P_6); 8.18 (s, 1H, T_A); 8.09 (td, 2H, $T_{44''}$); 7.99 (d, 1H, P_3); 7.89 (m, 1H, T_C); 7.83 (d, 2H, P_9); 7.81 (m, 1H, T_E); 7.74 (m, 4H, $T_{66''} + T_a$); 7.68 (m, 1H, T_D); 7.50 (m, 2H, $P_3 + B_p$); 7.34 (m, 4H, $B_o + T_{55''}$); 7.21 (d, 2H, P_a); 7.05 (d, 2H, T_b); 6.90 (m, 4H, $P_b + B_m$); 6.71 (s, 2H, P_m); 4.05 (t, 2H, α_T); 3.86 (t, 2H, α_P); 2.14 (s, 6H, Me°); 1.59 (s, 3H, Me^p); 1.81 (m, 2H, β_T); 1.69 (m, 2H, β_P); 1.53−1.17 (m, 28H, $\gamma_P - \iota_P + \gamma_T - \iota_T$). ES-MS *m*/*z* (calcd): 623.28 (623.27, $[M - 2PF_6]^{2+}$); 1391.53 (1391.50, $[M - PF_6]^+$).

21_{th}^{2+}. A 21 mg (14 μmol) amount of [**17_{photo}**][PF_6]$_2$ was dissolved in 2 mL of distilled DMSO, put under argon, and heated in the dark at 140 °C for 2 h. The complex was precipitated with KPF_6, filtered, washed with water, recovered with acetone, and dried. A 5 mL amount of acetonitrile was added, and the solution was flushed with argon and refluxed for 2 h under argon and in the dark. KPF_6 was added until complete precipitation, and the solid was filtered, washed with water, recovered with acetone, and dried. Column chromatography on 150 mL of silica gel (eluent, acetone/water/KNO_3 80:5:0.5) yielded 17 mg of [**21_{th}**][PF_6]$_2$ (84%). ^{1}H NMR 500 MHz (δ (ppm) in CD_2Cl_2): 9.81 (d, 1H, P_9, J = 1.8 Hz); 8.93 (d, 1H, P_7, J = 1.8 Hz); 8.48 (d, 1H, P_4, J = 8.1 Hz); 8.43 (d, 1H, P_6); 8.37 (d, 2H, $T_{33''}$); 8.26 (s, 2H, $T_{3'5'}$); 8.23 (d, 1H, P_5, J = 8.8 Hz); 8.03 (td, 2H, $T_{44''}$, J = 7.7,1.5 Hz); 7.94 (d, 2H, P_a, J = 8.8 Hz); 7.90 (m, 1H, T_E); 7.84 (m, 2H, $T_A + T_C$); 7.78 (m, 1H, T_D); 7.69 (d, 2H, T_a); 7.48 (d, 2H, $T_{66''}$); 7.30 (m, 3H, $P_3 + T_{55''}$); 7.17 (d, 2H, P_b, J = 8.8 Hz); 7.02 (d, 2H, T_b, J = 8.8 Hz); 6.58 (s, 2H, P_m); 4.14 (t, 2H, α_P, J = 7.0 Hz); 4.09 (t, 2H, α_T, J = 6.6 Hz); 2.20 (s, 3H, Me^p); 2.07 (s, 3H, AN_{Me}); 1.75 (m, 4H, $\beta_T + \beta_P$); 1.39 (4H, $\gamma_T + \gamma_P$); 1.30−1.10 (m, 24H, $\delta_T - \iota_T + \delta_P - \iota_P$); 0.85 (s, 6H, Me°). HR ES MS *m*/*z* (calcd): 1329.490 (1329.488, $[M - PF_6]^+$). UV−vis (λ_{max} (ϵ in L mol^{-1} cm^{-1}) in acetone): 462 nm (14 700).

22_{th}^{2+}. A 25 mg (17 μmol) amount of [$\mathbf{17}_{photo}$][PF_6]$_2$ was dissolved in 4 mL of distilled DMSO, put under argon, and heated in the dark at 140 °C for 2 h. The complex was precipitated with KPF_6, filtered, washed with water, recovered with acetone, and dried. A 50 mg amount of tetraethylammonium chloride and 10 mL of acetone were added; the solution was put under argon, refluxed for 3 h, and let cool to room temperature overnight. KPF_6 was added until complete precipitation; the solid was filtered, washed with water, recovered with acetone, and dried. Column chromatography on 160 mL of silica gel (eluent, acetone/water/KNO_3 80:5:0.5) yielded 23 mg of [$\mathbf{22}_{th}$][PF_6]$_2$. Yield: 100%. ^{1}H NMR 500 MHz (δ (ppm) in acetone-d_6): 10.94 (d, 1H, P_9, J = 1.8 Hz); 9.18 (d, 1H, P_7, J = 1.8 Hz); 8.71 (d, 2H, $T_{33''}$); 8.66 (s, 2H, $T_{3'5'}$); 8.62 (d, 1H, P_4, J = 8.1 Hz); 8.57 (d, 1H, P_6); 8.40 (d, 1H, P_5, J = 8.8 Hz); 8.13 (m, 1H, T_E); 8.02−7.95 (m, 5H, $T_{44''}$ + P_a + T_A); 7.83 (m, 1H, T_C); 7.78 (m, 1H, T_D); 7.73 (m, 4H, T_a + $T_{66''}$); 7.37 (d, 1H, P_3); 7.25 (m, 2H, $T_{55''}$); 7.22 (d, 2H, P_b, J = 8.8 Hz); 7.06 (d, 2H, T_b, J = 8.8 Hz); 6.64 (s, 2H, P_m); 4.21 (t, 2H, α_P, J = 7.0 Hz); 4.16 (t, 2H, α_T, J = 6.6 Hz); 2.20 (s, 3H, Me^p); 1.76 (m, 4H, β_T + β_P); 1.42 (4H, γ_T + γ_P); 1.30 (m, 4H, δ_T + δ_P); 0.90 (s, 6H, Me°). ES-MS *m*/*z* (calcd): 1178.462 (1178.465, [M − PF_6]$^+$). UV−vis (λ_{max} (ϵ in L mol^{-1} cm^{-1}) in acetone): 512 nm (11 600).

23_{th}^{2+}. A 6 mg (4 μmol) amount of [$\mathbf{17}_{photo}$][PF_6]$_2$ was put in an NMR tube and dissolved in deuterated DMSO. The tube was closed with a normal stopper, and a reference spectrum was taken. The tube was heated in the dark at 140 °C for 2 h. After cooling to room temperature, a spectrum was taken showing complete isomerization of the macrocycle and removal of pyridine, giving a 66:33 mixture of products analyzed as S-bonded:O-bonded [$\mathbf{23}_{th}$]-[PF_6]$_2$, respectively. After one night at room temperature in the dark the mixture evolved to a 87:13 ratio, which enabled analysis of the main product (S-bonded [$\mathbf{23}_{th}$][PF_6]$_2$). ^{1}H NMR 300 MHz (δ (ppm) in DMSO-d_6): 10.67 (d, 1H, P_9); 9.42 (d, 1H, P_7); 8.88 (d, 2H, $T_{33''}$); 8.85 (s, 2H, $T_{3'5'}$); 8.83 (d, 1H, P_4); 8.59 (d, 1H, P_6); 8.45 (d, 1H, P_5); 8.23 (td, 2H, $T_{44''}$); 8.21 (m, 1H, T_E); 8.01 (m, 3H, P_a + T_A); 7.92−7.76 (m, 6H, T_C + T_D + T_a + $T_{66''}$); 7.46 (m, 3H, P_3 + $T_{55''}$); 7.26 (d, 2H, P_b); 7.10 (d, 2H, T_b); 6.53 (s, 2H, P_m); 4.18 (m, 4H, α_P + α_T); 2.13 (s, 3H, Me^p); 2.10 (s, 6H, $DMSO_{CH3}$); 1.68 (m, 4H, β_T + β_P); 1.42−1.10 (28H, $\gamma_{T\,-}$ ι_T + $\gamma_{P\,-}$ ι_P); 0.94 (s, 6H, Me°). ES-MS *m*/*z* (calcd): 571.745 (571.748, [M − DMSO − 2PF_6]$^{2+}$); 609.74 (610.755, [M − H − 2PF_6]$^{2+}$); 1222.4 (1221.5, [M − H − PF_6]$^+$). UV−vis (λ_{max} in acetone): 438 (S-bonded) and 496 nm (O-bonded).

Acknowledgment. We thank the CNRS for financial support. The Région Alsace is also gratefully acknowledged for a fellowship to S.B. We also thank Johnson Matthey Inc. for a loan of $RuCl_3$.

Supporting Information Available: X-ray crystallographic data for $\mathbf{10}_{th}^{2+}$; synthesis and characterization of **4** and **5** (S1,S2); ^{13}C NMR data of the ruthenium complexes (S2,S6); electronic spectra of $\mathbf{10}_{th}^{2+}$ and $\mathbf{10}_{photo}^{2+}$ (S6); thermo- and photoprocesses for a stripped down version of $\mathbf{8}_{th}^{+}$ (S7,S10). This material is available free of charge via the Internet at http://pubs.acs.org.

IC700734Q